Photoactivity of new octacationic Mg^{II} and Zn^{II} porphyrazines in water solution and G-quadruplex binding ability of differently sized Zn^{II} porphyrazines

Fabiola Sciscione,[a] Francesco Manoli,[b] Elisa Viola,[a] Jitendra Wankar,[b] Claudio Ercolani,[a] Maria Pia Donzello,[a]* and Ilse Manet[b]*

[a] Dipartimento di Chimica, Università La Sapienza, P.le A. Moro 5, 00185 Roma, Italy
[b] Istituto per la Sintesi Organica e la Fotoreattività(ISOF), Consiglio Nazionale delle Ricerche (CNR), Via Gobetti 101, 40129 Bologna, Italy

Abstract

The new octacations $[(2\text{-Mepy})_8PzM]^{8+}$ (M = $Mg^{II}(H_2O)$, Zn^{II}), isolated as iodide salts, were obtained from the corresponding neutral complexes $[Py_8PzM]$ (Py = 2-pyridyl; Pz = porphyrazinato dianion) upon quaternization with CH_3I of the N atoms of the 2-pyridyl rings under mild experimental conditions. The absorption spectra registered in organic solvents as well as in water confirm the presence of the complexes in their monomeric form in all cases. The two octacations behave as photosensitizers in H_2O/SDS solution for the production of singlet oxygen, $^1O_2$, and exhibit quantum yields values (Φ_Δ), 2.3-2.5 higher than those measured for the standard $PcAlS_{mix}$, a promising feature of interest for photodynamic therapy (PDT). The interaction of the Zn^{II} octacationic complex $[(2\text{-Mepy})_8PzZn]^{8+}$ with different types of DNA has been studied by means of optical spectroscopic techniques clearly suggesting that binding of the charged macrocycle to the DNA effectively takes place. In order to assess the effect of the aromatic ring size, the same binding study was performed for the octapyridinated tetraquinoxalinoporphyrazine Zn^{II} complex having a much more expanded macrocyclic framework and compared with the behaviour of the parent octapyridinated tetrapyrazinoporphyrazine Zn^{II} complex having an intermediate macrocycle. The achieved information confirms the relationship between binding of the charged macrocycle to the DNA and the dimension of the porphyrazine macrocycle.

Introduction

Recently we reviewed[1] the synthetic procedures and structural features of the porphyrazine macrocycles tetrakis[di(2-pyridyl)pyrazino]porphyrazines, [TPyzPzM] Scheme 1A (M = $2H^I$, bivalent metal centers),[2] the parent bi/pentanuclear species[2c,d,e,3,4,5] and their mononuclear octacationic[2c,d,e,6] (Scheme 1B) and heterobinuclear hexacationic[3] metal derivatives bearing one

exocyclic *cis*-platin-like $N_{2(Py)}PtCl_2$ functionality (Scheme 1C). The pluricharged species are of great interest because, differently from the neutral related macrocycles, they are all soluble in water up to 10^{-5} M or even higher concentrations, thus opening the route to biochemical investigations in this medium. In this regard, we aim at implementing multiple functionalities in one single molecule, like (i) near-IR (NIR) light triggered production of singlet oxygen, $^1O_2$, for application in photodynamic therapy (PDT); (ii) activity as stabilizing ligand of G-quadruplex structures of guanine-rich DNA sequences; (iii) intrinsic NIR fluorescence useful for imaging purposes and (iv) chemotherapeutic activity thanks to the presence of cis-platin-like groups, $N_{2(py)}PtCl_2$.

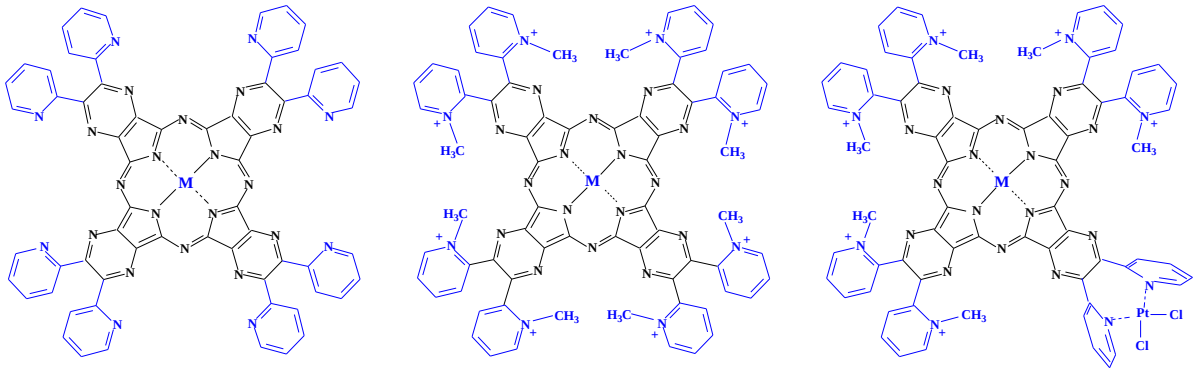

A BC

Scheme 1. A) $[Py_8TPyzPzM]$, B)$[(2\text{-}Mepy)_8TPyzPzM]^{8+}$ (M = $2H^I$, bivalent metal ions)and C) $[(PtCl_2)Py_2(2\text{-}Mepy)_6TPyzPzM]^{6+}$ (M = bivalent metal ions).

As reported in detail, several metal derivatives of the TPyzPz macrocycle in their neutral or cationic form, incorporating centrally Zn^{II}, Mg^{II}, Pd^{II} or Pt^{II}, were able to act as photosensitizers for singlet oxygen production with high quantum yields (Φ_Δ) in DMF or DMF/HCl, where they are present in their monomeric form.[2e,4,5,7] Moreover, the mononuclear Zn^{II} octacation $[(2\text{-}Mepy)_8TPyzPzZn]^{8+}$ (Scheme 1B) and the related heterobimetallic Zn^{II}/Pt^{II}hexacation $[(PtCl_2)Py_2(2\text{-}Mepy)_6TPyzPzZn]^{6+}$ (Scheme 1C) were alsoable to act as G-quadruplex stabilizing ligands in water. Both complexes, although partially aggregated, in K^+ rich water solution form stable (porphyrazine:DNA) complexes with the telomeric sequence 5'-d[AGGG(TTAGGG)$_3$]-3' adopting a G-quadruplex structure.[8a,b] This oligomer has been chosen as model of guanine(G)-rich sequences adopting G-quadruplex structures. G-rich sequences are present in very important regions of the human genome, like the telomeres at the end of the chromosomes and the promoter regions of several oncogenes.[9] There is increasing evidence now of their existence *in vivo* and druggability thus boosting the search

for molecules able to interact with this secondary DNA structure.[10] More recently we reported that both cations are able to form non covalent complexes with a model of B-DNA.[11] Aggregation of the two cations could be disrupted both upon addition of DNA as well as SDS micelles to the porphyrazine in a water solution, and the almost exclusive presence of monomeric species in water/SDS resulted in improved photoactivity of interest for PDT.[12] In addition, the two cations evidenced in aqueous media anticancer effects on the melanoma C8161 and the oral squamous carcinoma CA-1 cell lines.[12]

Lately, we synthesized and characterized new neutral porphyrazine compounds ([Py_8PzM], with M = $Mg^{II}(H_2O)$[13] and Zn^{II}), with a smaller aromatic core than that of the pyrazinoporphyrazine macrocycles in Scheme 1A, bearing externally 2-pyridyl rings directly appended to the pyrrole rings of the tetrapyrrolic core.[14]With the aim of promoting solubility in water as monomers we addressed our efforts to the preparation of the octacations $[(2\text{-Mepy})_8PzM]^{8+}$ with M = $Mg^{II}(H_2O)$, Zn^{II} (see Scheme 2A), isolated as iodide salts, obtained from the respective neutral complexes [Py_8PzM] by reaction with CH_3I under mild experimental conditions. The two new charged macrocycles are present exclusively in their monomeric form in water, where they exhibit good solubility which is of great relevance for the photoactivity and cell permeability of the two octacations. The behaviour of the two complexes as potential $^1O_2$ sensitizers for PDT has been examined in water solution, and in a non aqueous solvent (DMF). Further we investigated the DNA binding behaviour of the Zn^{II} and Mg^{II} octacationic species. In order to assess the importance of the size of the macrocyclic ring in DNA binding, we compared the data obtained for the smaller Zn^{II} complex $[(2\text{-Mepy})_8PzZn]^{8+}$ (Scheme 2A) with those of the intermediate π-extended pyrazinoporhyrazine octacation $[(2\text{-Mepy})_8TPyzPzZn]^{8+}$ (Scheme 1B; M = Zn^{II})[8a,b,11] and completed the study with an investigation of the DNA binding of the recently reported[15] quinoxalinoporphyrazine Zn^{II} complex $[(2\text{-Mepy})_8QxPzZn]^{8+}$ (Scheme 2B). The interaction of the complexes with different types of DNA assuming both G-quadruplex (G4) and duplex structure has been investigated by means of steady-state and time-resolved optical spectroscopy. The study clearly shows that association of the charged macrocycle to the DNA occurs and gives some clues on the importance of the size of the macrocycle.

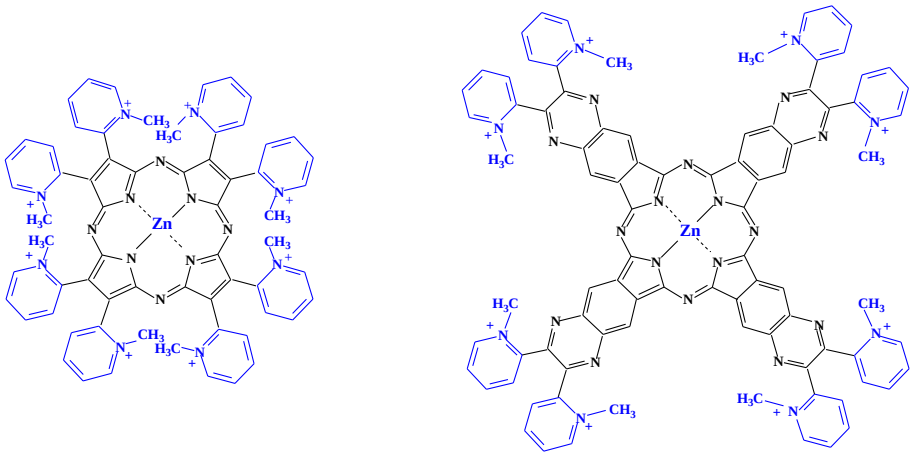

A B

$[(2\text{-Mepy})_8\text{PzZn}]^{8+}[(2\text{-Mepy})_8\text{QxPzZn}]^{8+}$

Scheme 2

Experimental Section

Solvents and reagents were used as purchased,unless otherwise specified. Pyridine, dried by refluxing over CaO, and dimethyl sulfoxide (DMSO, RPE C. Erba), freshly distilled over CaH_2, were used for the spectroscopic measurements. The Mg^{II} complex $[Py_8PzMg(H_2O)]\cdot xH_2O$ (x = 4-6) was prepared following the previously reported procedure[13] or slightly modifying its purification as outlined in recent report.[14]and information on the composition and structure of the Mg^{II} complex were adequately defined based on elemental analyses and detailed NMR spectra in DMF-d_7,[13]recorded also in DMSO-d_6.[14] The Zn^{II} analog $[Py_8PzZn]\cdot xH_2O$ (x = 3-6) was prepared via a transmetalation process from the Mg^{II} complex by reaction with $Zn(OAc)_2\cdot 2H_2O$ in glacial CH_3COOH with stirring at room temperature for 5 h, as reported elsewhere.[14] The Zn^{II} octacationic porphyrazine macrocycle with external quinoxaline fragments (formula shown in Scheme 2B), isolated as iodide salt, was prepared as described elsewhere.[15]9,10-Anthracenediylbis(methylene)malonic acid and sodium dodecyl sulphate (SDS) were purchased from Sigma Aldrich. H_2O Millipore was used as solvent. $PcAlS_{mix}$ was kindly provided by Prof. E. I. Lukyanets. The DNA sequences, 5'-d[AGGG(TTAGGG)$_3$]-3' (hTel22), 5'-[$GAG_3TG_4AG_3TG_4AAG$]-3' (c-myc2345) and the self-complementary 5'-[$CA_2TCG_2ATCGA(AT)TCGATC_2GAT_2G$]-3' (ds26mer) have been acquired from Sigma-Aldrichand used as received.

Synthesis of [(2-Mepy)$_8$PzMg(H$_2$O)](I)$_8$·6H$_2$O. The complex [Py$_8$PzMg(H$_2$O)]·5H$_2$O (32.0mg, 0.030 mmol) and CH$_3$I (0.20 mL, 3.21 mmol) were added to DMF (1 mL) and the mixture was kept under stirring at room temperature for 20 h. After evaporation of excess CH$_3$I in air at room temperature, DMF was distilled under vacuum (10^{-2} mmHg). The solid bluish residue was washed with ether and brought to constant weight under vacuum (45.0 mg, yield 68%). Calcd for [(2-Mepy)$_8$PzMg(H$_2$O)](I)$_8$·6H$_2$O, C$_{64}$H$_{70}$I$_8$MgN$_{16}$O$_7$: C, 34.71; H, 3.19; N, 10.12. Found: C, 34.32; H, 3.22; N, 10.39%. IR (KBr, cm^{-1}): 3420 (broad),2979 (m),1734 (w), 1685 (vw), 1626 (w), 1578 (w), 1510 (w), 1467 (w), 1424 (vw), 1399 (w-m), 1275 (w-m), 1185 (w), 1151 (w), 1121 (w), 1093 (w-m), 1039 (w, 1005 (w-m), 984 (w-m), 943 (w), 889 (w), 877 (w-m), 855 (w-m), 829 (w), 771 (m-s), 740 (m), 709 (s), 623 (w).

Synthesis of [(2-Mepy)$_8$PzZn](I)$_8$·7H$_2$O. [Py$_8$PzZn]·5H$_2$O (23.0 mg, 0.021 mmol) and CH$_3$I (0.18 mL, 2.89 mmol) were added to DMF (1 mL) and the mixture was kept under stirring at room temperature for 20 h. After evaporation of excess CH$_3$I, DMF was distilled under vacuum (10^{-2}mmHg). The solid bluish material was washed with ether and brought to constant weight under vacuum (35.0 mg, yield 74%). Calcd for [(2-Mepy)$_8$PzZn)](I)$_8$·7H$_2$O, C$_{64}$H$_{70}$I$_8$N$_{16}$O$_7$Zn: C, 34.07; H, 3.13; N, 9.93; Zn, 2.90. Found: C, 33.87; H, 3.44; N, 10.25; Zn 3.10%. IR (KBr, cm^{-1}): 3410 (broad), 2973 (m), 2807 (vw), 2757 (w), 1627 (s), 1578 (w), 1551 (w), 1506 (w), 1467 (w), 1401 (vw), 1373 (w), 1277 (w), 1185 (w), 1158 (w), 1092 (w), 1076 (w), 1046 (w), 1004 (w-m), 985 (m), 953 (w), 913 (w), 879 (w-m), 855 (w), 833 (w-m), 767 (w), 721 (w), 689 (w).

Singlet Oxygen Photoproduction in Water Solution. Measurements on the efficacy of [(2-Mepy)$_8$PzZn]$^{8+}$ and [(2-Mepy)$_8$PzMg(H$_2$O)]$^{8+}$ in the production of ^{1}O$_2$ were performed in aqueous solution using PcAlS$_{mix}$ as reference standard (Pc: phthalocyaninato dianion, [C$_{32}$H$_{16}$N$_8$]$^{=}$). The alternative use of the Zn^{II} analog, PcZnS$_{mix}$, for the same purposes was discouraged by the fact that it might show a higher degree of aggregation in water solution,[16]as was directly verified by us. PcAlS$_{mix}$ is a mixture of compounds with different sulfonation degree and different isomers having formula PcAlOH(SO$_3$Na)$_n$ with <n> ~ 3. PcAlS$_{mix}$ is a well-known singlet oxygen sensitizer, commercially known as Photosens® presently in clinical use in Russia. A sample of PcAlS$_{mix}$ with <n> ~ 3 was a kind gift by Prof. E. A. Lukyanets.[17] The complex is monomeric in water solution and gives reproducible experiments and, on this basis, it can be used for comparison purposes in

singlet oxygen quantum yield measurements in H_2O on phthalocyanine or porphyrazine macrocycles.[18,19] The sample was recently tested by us with success in reported similar experiments.[12]

The efficacy of the two cations $[(2\text{-Mepy})_8PzZn]^{8+}$ and $[(2\text{-Mepy})_8PzMg(H_2O)]^{8+}$ as $^1O_2$ photosensitizers was examined by analyzing the decomposition of the scavenger ADMA (tetrasodium-9,10-anthracenediylbis(methylene)malonate) obtained from the corresponding acid salted with NaOH up to pH ~ 7, and proved to be a specific and very reactive probe for $^1O_2$ detection in aqueous media.[18,20,12] A profile of the procedure used for the studied species, including $PcAlS_{mix}$, is as follows.

A water solution (2.0 mL) of the monomeric photosensitizer (c ~ 4×10^{-6} M; absorbance ~0.4 at the wavelength of irradiation) containing the anionic surfactant SDS (H_2O/SDS; [SDS] = 0.020 M; as to the role of SDS see the later discussion) and the scavenger ADMA (c ~ 1×10^{-4} M) was irradiated in a 1.0 cm-quartz cell by a laser source (Premier LC Lasers/HG Lens, Global Laser) in the region of the Q band (λ_{irr} = 670 nm). Illumination was directed normally both to the surface of the solution and to the spectrophotometric radiation. During the experiment, continuous magnetic stirring ensured homogeneity of the solution while a circulating water system kept the temperature constant at 30°C. The power of irradiation (*W*), accurately measured by a radiometer (ILT 1400A/SEL100/F/QNDS2, International Light Technologies), was fixed at ca. 5 mW. The pH of the solution was in the range 6.5-7.0 and no changes of its value were observed after irradiation.

The decay of scavenger's absorption at 380 nm was monitored as a function of the time, and sensitizer stability was also checked under irradiation. Because of the fast decay of $^1O_2$ in aqueous solution, the photo-oxidation of the scavenger ADMA, under the experimental conditions described above, follows a first-order kinetic equation.[21] The relative photosensitizing activity of the present Zn^{II} and Mg^{II} cationic species in the production of singlet oxygen with respect to the reference $PcAlS_{mix}$ was determined on the basis of the following equation:

$$\textit{Relative photosensi tizing activity} = \frac{k_I W_{abs}^R}{k_I^R W_{abs}} \qquad (1)$$

where k_I and k_I^R are the ADMA bleaching first-order rate constants of octacation and the reference $PcAlS_{mix}$, respectively; W_{abs} and W_{abs}^R are the rate of light absorption by the examined cation and

the reference, respectively, calculated considering an optical path length of 2.1 cm (total volume of solution and magnet in the cuvette = 2.1 mL; $W_{abs} = W\,(1\times10^{-2.1\,A})$.[22]

Other Physical Measurements. IR spectra of the solid materials as KBr pellets were recorded in the range of 4000-600 cm^{-1} on a Varian 660-IR FT-IR spectrometer. UV-visible solution spectra other than those for spectral studies on the interaction of the Zn^{II}octacation with the G4 quadruplex structure and ds DNA (see below) were recorded on a Varian Cary 5E spectrometer by using 1-cm quartz cuvettes. Elemental analyses for C, H, and N were provided by the "Servizio di Microanalisi" at the Dipartimento di Chimica, Università "Sapienza" (Rome) on an EA 1110 CHNS-O instrument. The ICP-PLASMA analysis for Zn was performed on a Varian Vista MPX CCD simultaneous ICP-OES.

Sample preparation for DNA binding study. The buffer for the spectroscopic measurements contained 10 mM K-phosphate, and 100 mM KCl. Excess of K^+ mimics physiological conditions of cellular compartments where K^+ is abundant. pH was corrected to a value of 7.0 with aliquots of HCl 3N. For melting experiments a 10 mM phosphate buffer with 100 mMKCl was used with pH corrected to a value of 7.0 with HCl 0.1 N. Three different DNA sequences were used: a telomeric DNA sequence, 5'-[$AG_3(T_2AG_3)_3$]-3' indicated as hTel22, part of the *c-Myc* gene promoter sequence, 5'-[$GAG_3TG_4AG_3TG_4AAG$]-3' indicated as c-myc2345, and a self-complementary sequence, 5'-[$CA_2TCG_2ATCGA(AT)TCGATC_2GAT_2G$]-3' indicated as ds26mer adopting a double stranded (ds) DNA structure in solution. Concentration of DNA was determined spectrophotometrically at 260 nm using the values 228.500 $M^{-1}cm^{-1}$, 232.000 $M^{-1}cm^{-1}$ and 414.000 $M^{-1}cm^{-1}$ for hTel22, c-myc2345 and ds26mer in its hybridized form, respectively.The DNA stock solution was heated at 90 °C for 15 min and then cooled down to room temperature before use. The iodide salt of $[(2\text{-Mepy})_8PzZn]^{8+}$ was dissolved up to a concentration of 1.2×10^{-5} M in these buffers. Aliquots of solution of the charged macrocycle and DNA solution in the same buffer were mixed together to prepare samples of varying molar ratio. Water was purified by passage through a Millipore MilliQ system (Millipore SpA, Milan, Italy).

Titration experiments. Titrations at constant ligand and varying DNA concentrations were performed monitoring absorption, circular dichroism (CD) and fluorescence. All the measurements were carried out at 295 K. Absorption spectra in the 220-850 nm range were recorded on a Perkin

Elmer λ 650 spectrophotometer. CD spectra were obtained with a Jasco J-715 spectropolarimeter. Quartz cuvettes were used with optical path of 0.2, 1 or 2 cm depending on the DNA concentration. CD spectra in the 210-315 nm range were registered accumulating 4 scans with integration time of 1 s and 1 nm steps.Visible CD spectra were registered in 2 cm cuvette accumulating 3 scans in the 330-480 nm region and 4 scans in the 590-700 nm region with integration time of 1 s and 1 nm steps.Scan rate was 50 nm/min and band width of 2 nm was applied. Fluorescence spectra were measured using 1 nm steps and 1 s dwell time. Slits were kept narrow to 3-4 nm band width in excitation and emission. Right angle detection was applied. The measurements were carried out in quartz cuvettes with path length of 1 cm. All fluorescence spectra have been obtained for air-equilibrated solutions absorbing less than 0.12 at all wavelengths to avoid inner filter effects and re-absorption of emission. Furthermore, they have been corrected for wavelength dependent response of the monochromator/PMT couple. Fluorescence decays in air-equilibrated solution were collected upon excitation at 637 nm with a Hamamatsu pulsed laser with 1 MHz repetition rate using a time-correlated single photon counting system (TCSPC) (IBH Consultants Ltd., Glasgow, UK) with a time interval of 55 ps per channel. Photons were detected at 680 nm in right angle configuration with a 645 nm cut-off filter. Fluorescence decay profiles were analyzed with a least-squares method, using multiexponential decay functions and deconvolution of the instrumental response function. The software was provided by IBH Consultants Ltd. Lifetime resolution of the system is 0.2 ns.

The function used to fit the fluorescence decay is:

$$I(t) = b + \Sigma_j a_j e^{(-t/\tau j)} \qquad (2)$$

The relative amplitude, also known as the fractional intensity, and the average fluorescence lifetime are calculated according to the following equations:

$$f_i = a_i\tau_i / \Sigma_j a_j\tau_j \qquad (3) \qquad \tau_{av} = \Sigma_j f_j\tau_j \qquad (4)$$

After titration experiments the best complexation model and the related association constants were determined by global analysis of multiwavelength data sets corresponding to spectra of different mixtures, using the commercially available program Reactlab[@] distributed by JPlus Consulting.[23]The multivariate optimization procedure is based on Singular Value Decomposition (SVD) and non linear regression modelling by the Levenberg-Marquardt algorithm. The deviations

of the calculated absorbance, fluorescence intensity/ellipticity from the experimental values were minimized in a completely numerical procedure.

DNA Melting experiments. DNA melting was monitored by means of absorption or circular dichroism at fixed wavelengths. As to the absorption experiment for hTel22 melting a temperature gradient of 30°C/hr was used monitoring absorbance at 260 and 295 nm using a bandpass of 1 nm and reading absorbance every 0.5°C.In the case of DNA melting in the presence of porphyrazine ellipticity was measured with increasing temperature. A temperature gradient of 12°C /hr was appliedand ellipticity was read every 1°C. A bandwidth of 2 nm and a response time of 8 seconds at 260 and 295 nm in K^+ rich solutions were applied.

Results and Discussion

Synthetic aspects and solid state properties of the complexes [(2-Mepy)$_8$PzM](I$_8$)·xH$_2$O (M = Mg^{II}(H$_2$O), Zn^{II}). The title complexes can be obtained in high yields as stable-to-air bluish-green solids from the corresponding neutral complexes [Py$_8$PzM]·xH$_2$O by quaternization of the pyridine N atoms using CH_3I in DMF under mild experimental conditions, this leading to the formation of the octacations $[(2\text{-Mepy})_8PzMg(H_2O)]^{8+}$ and $[(2\text{-Mepy})_8PzZn]^{8+}$. Similarly to the neutral species,the Mg^{II} macrocyclic octacation is formulated with one axially ligated water molecule, as strongly supported by the literature data on phthalocyanine and porphyrazine Mg^{II} complexes reported in detail in ref. 13.The IR spectra of the two charged species do not differ significantly from the spectra of the parent neutral species, the only exception being weak-to-medium intensity peaks observed in the region 3000-2700 cm^{-1} which are assigned to the presence of the external CH_3 groups. The two salt-like species share solubility in the polar solvents pyridine, DMSO, and DMF comparable to that of the corresponding neutral species [Py$_8$PzM]. Importantly, the octacationic macrocycles as iodide salts have solubility in water of 10^{-5} M concentration or higher, which is of primary interest for the envisaged applications.

UV-Visible Absorption spectra in Nonaqueous Solvents and in Water. The UV-visible absorption spectrum of the Zn^{II} complex immediately after dissolution in DMF (Figure 1, black line; c = 10^{-5}-10^{-6} M) is characterized by a featureless region between 300 and 700 nm and the presence of a Q-band peak at 732 nm. The spectrum resembles that observed for several neutral or

charged macrocyclic pyrazinoporphyrazine analogs, either seen electrochemically upon one-electron uptake [2b,c,d,6] or by reduction occurring in DMF at the appropriate solution concentration (ca. 10^{5}-10^{-6} M),[2e,3,4,7]thus forming their corresponding -1 charged species. Assignment of the observed spectrum in the present study to the cationic species $[(2\text{-Mepy})_8\text{PzZn}]^{7+}$ is further supported by the compound's reoxidation to the corresponding octacation $[(2\text{-Mepy})_8\text{PzZn}]^{8+}$ upon addition of HCl (ca. 10^{-4} M) as evidenced by the concomitant reverse spectral change (Figure 1, red line).[7] A stable spectrum of the unreduced species is easily seen in DMF in the presence of pre-added HCl (10^{-4} M). The spectrum shows Soret and Q bands, with respective peaks at 384 and 653 nm, indicative of the presence of the octacation in its monomeric form. A much slower one-electron reduction process also occurs in DMF for the corresponding Mg^{II} octacation and a similar reoxidation can be accomplished by the addition of HCl to solution. A parallel reduction process (slow, >>24 hrs) can be spectrally observed for both cations in pyridine but only for the Zn^{II} complex in DMSO, in which solvent the Mg^{II} complex appears to be stable with time. Table 1 summarizes the UV-visible spectral data of the two cations in non-aqueous solvents and in water solution.

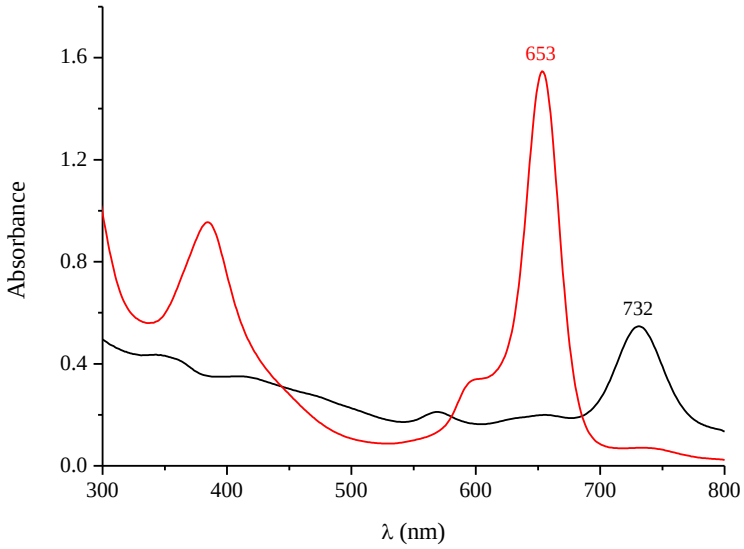

Figure 1. UV-visible spectra $[(2\text{-Mepy})_8\text{PzZn}]^{8+}$in DMF (black line) and in DMF/HCl (red line).

Table 1. UV-visible spectral data (λ, nm (log ε)) of the octacations $[(2\text{-Mepy})_8PzM]^{8+}$and the related neutral compounds $[Py_8PzM]$(M = Zn^{II}, $Mg^{II}(H_2O)$)in different solvents.

Compound	Solvent	Soret region	Q-band region		Ref.
$[(2\text{-Mepy})_8PzZn]^{8+}$	DMF/HCl[a]	384 (4.66)	596sh (4.19)	653 (4.87)	tw
	DMSO	381 (4.66)	596sh (4.19)	656 (4.86)	tw
	Py[b]	386	598	659	tw
	H_2O	376 (4.78)	581sh (4.26)	641 (4.90)	tw
	H_2O/SDS[c]	381 (4.81)	595sh (4.29)	651 (4.94)	tw
$[Py_8PzZn]$	DMF	380 (4.82)	585 (4.26)	637 (4.98)	14
	DMSO	380 (4.92)	584 (4.35)	636 (5.07)	14
	py	381 (4.85)	583 (4.27)	637 (4.97)	14
$[(2\text{-Mepy})_8PzMg(H_2O)]^{8+}$	DMF	382 (4.67)	597sh (4.24)	658 (4.88)	tw
	DMF/HCl[a]	375 (3.98)	592sh (3.38)	651 (3.82)	tw
	DMSO	381 (4.77)	596sh (4.27)	656 (4.96)	tw
	py	385 (4.75)	598sh (4.25)	657 (4.91)	tw
	H_2O	376 (4.74)	584sh (4.24)	643 (4.85)	tw
	H_2O/SDS[d]	380 (4.53)	597sh (4.20)	651 (4.63)	tw
$[Py_8PzMg(H_2O)]$	DMF	378 (5.05	583 (4.46	636 (5.18	13
	DMSO	378 (4.52	583 (3.95	636 (4.63	13
	py	381 (4.80	583 (4.18	638 (4.89	13

[a]Solution in DMF with HCl ($c = 2 \times 10^{-4}$ M).
[b] Unstable spectrum (see discussion in the text).
[c] SDS = sodium dodecyl sulphate c = 0.020 M in water solution.
[d] Solution in DMF ($c \geq 10^{-5}$ M).

Comparison of the spectral data for the octacationic species $[(2\text{-Mepy})_8PzM]^{8+}$ (M = Zn^{II}, $Mg^{II}(H_2O)$) in the examined non-aqueous solvents (pyridine, DMSO, DMF) with those of the corresponding neutral complexes $[Py_8PzM]$, shows that there is a 20 nm bathochromic shift of the Q band in the direction neutral → octacationic species (Table 1). This indicates a decrease in energy of the related HOMO-LUMO transition and must be ascribed to an enhancement of the electron

deficient properties of the macrocycle due to quaternization of the pyridine N atoms, as was earlier observed for the pyrazinoporphyrazine analogs.[2c,d,6]

It is interesting that the UV-visible spectra of the cations $[(2\text{-Mepy})_8\text{PzM}]^{8+}$ (M = Zn^{II}, $Mg^{II}(H_2O)$) in pure water at c ≈ 10^{-5} M or lower are stable in time and show no evidence of aggregation. Both spectra are characterized by a maximum absorption at 376 nm in the Soret region and narrow intense Q bands at 641 and 643 nm for the Zn^{II} and Mg^{II} complexes, respectively (Zn^{II} complex in Figure 2, black line). This behavior is different from that observed for the more expanded pyrazinoporphyrazine octacations $[(2\text{-Mepy})_8\text{TPyzPzM}]^{8+}$.[6,8,11]For these latter macrocycles, a second band of comparable intensity is always present on the blue side of the Q band at concentrations of 10^{-5}-10^{-6} M, and this band has been assigned to an aggregated species which disappears upon dilution (10^{-7} M).[6,8,11]The absorption spectrum of the largest octacation $[(2\text{-Mepy})_8\text{QxPzZn}]^{8+}$ indicates the presence of high levels of aggregation in water solution (Figure 2, blue line), progressively disappearing in the presence of SDS, the final spectrum (Figure 2, red line) showing Soret and Q bands at 376 and 774 nm, respectively.

The presence of the two cations $[(2\text{-Mepy})_8\text{PzM}]^{8+}$ (M = Zn^{II} and $Mg^{II}(H_2O)$) in water in their monomeric form is of great importance in view of the potential biomedical applications of these species, *i.e.*, singlet oxygen sensitization in PDT, fluorescence imaging and the ability to interact with different DNA fragments, discussed below.

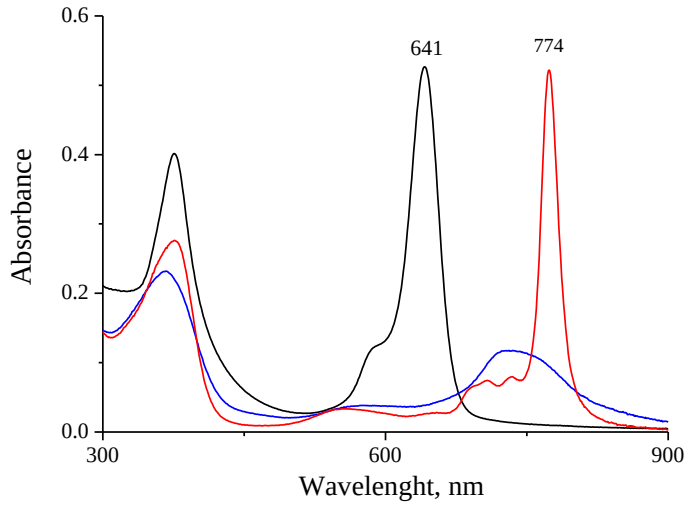

Figure 2. UV-visible spectraof$[\text{Py}_8\text{PzZn}]^{8+}$ in H_2O (black line) and of $[(2\text{-Mepy})_8\text{QxPzZn}]^{8+}$ in H_2O (blue line) and in H_2O in the presence of SDS (red line).

Singlet Oxygen Photoproduction in Water Solution. The experiments on the photosensitizing activity for the generation of $^1O_2$ of the cations $[(2\text{-Mepy})_8PzZn]^{8+}$ and $[(2\text{-Mepy})_8PzMg(H_2O)]^{8+}$ conducted in pure water showed no changes of the UV-visible spectrum expected for ADMA.The spectral changes accompanying the decomposition of the $^1O_2$ scavenger upon irradiation could be seen if the experiments were conducted in the presence of SDS. For both species addition of SDS resulted in a bathocromic shift (ca. 10 nm) of the Q-band maximum with no change of its intensity. Capture of the cationic species by SDS micelles reasonably avoided some type of electrostatic interaction present in solution between the anionic scavenger and the cationic photosensitizer, which negatively influences the experiment.

Following the comparative method described in the Experimental Section, the photodynamic potential was evaluated by comparing the ADMA bleaching first-order rate constants obtained for each one of the two species with that of the standard $PcAlS_{mix}$ determined under the same experimental conditions ([SDS] = 0.020 M; λ_{irr} = 670 nm). Figure 3 exemplifies the results of a typical experiment performed on the Zn^{II} octacation $[(2\text{-Mepy})_8PzZn]^{8+}$. Figure 3A shows the initial UV-visible spectrum of the solution containing the sensitizer (blue line, Q band at 651 nm) and the peaks of ADMA in the region 300-400 nm superimposed with the Soret band of the complex. Irradiation of the solution causes a complete disappearance of the ADMA peaks within 10 minutes. Figure 3B shows the ADMA-absorbance time decay at 380 nm which can be fitted according to a first-order law, thus allowing determination of the related *k* value. As can be seen, the absorbance of the Q band of the sensitizer, also checked during irradiation, remains constant during the experiment, indicating that the sensitizer is not undergoing photobleaching at all. The *k* values measured for coupled experiments conducted strictly under the same experimental conditions on the Zn^{II} or Mg^{II} species and the reference $PcAlS_{mix}$ were used in equation 1 to evaluate the relative photosensitizing activity of the studied cationic species.

The Φ_Δ values of $PcAlS_{mix}$ reported in the literature fall in the range $(0.34 \div 0.42) \pm 0.06$[24] and refer to different experimental conditions (in terms of medium composition, surfactant, irradiation range) than those required in the present comparative study for the reliable determination of the Φ_Δ values. For this reason we prefer to express the activity of the monomeric Mg^{II} and Zn^{II} cationic

complexes in water solution as "*relative photosensitizing activity*" compared to that shown by the reference standard $PcAlS_{mix}$, under the same experimental conditions.

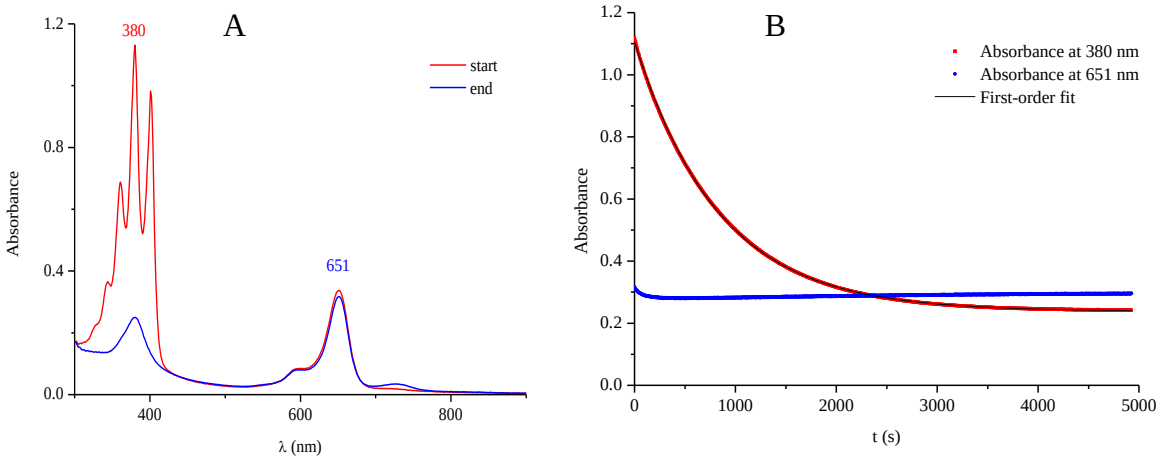

Figure 3. A) UV-visible spectra of $[(2\text{-Mepy})_8PzZn]^{8+}$and ADMA in H_2O+SDS ([SDS] = 0.020 M) before (red line) and after (blue line) laser irradiation; B) Absorbance values indicating ADMA photo-oxidation (red plot) and sensitizer Q-band maximum (blue dots) during irradiation; the related first-order exponential fit (black line) is also shown.

Table 2 lists the *relative photosensitizing activity* values for $^1O_2$ production measured for the present two cationic complexes in H_2O/SDS solutions. Noticeably, both cationic species in their monomeric form exhibit an efficiency for the production of $^1O_2$ in SDS water solution 2.2-2.5 times higher than that of the reference standard $PcAlS_{mix}$ arbitrarily fixed as 1. These data clearly propose the two cations as highly promising photosensitizers in PDT, deserving special attention in the context of the literature data reported on water soluble porphyrazine and phthalocyanine macrocyclic species.[16,19,25,26]

Table 2. Photochemical data for $[(2\text{-Mepy})_8PzZn]^{8+}$, $[(2\text{-Mepy})_8PzMg(H_2O)]^{8+}$, and $PcAlS_{mix}$ in H_2O/SDS.

Photosensitizer	Singlet Oxygen Production (λ_{irr} = 670 nm)	
	λ_{max} (nm)	Relative photosensitizing activity[a]
$[(2\text{-Mepy})_8PzZn]^{8+}$	651	2.5
$[(2\text{-Mepy})_8PzMg(H_2O)]^{8+}$	651	2.2
$PcAlS_{mix}$[b]	678	1

[a] Mean value of at least three measurements.
[b] The singlet oxygen quantum yield for $PcAlS_{mix}$ in posphate buffer has been reported to be in the range (0.34 ÷ 0.42) ± 0.06.[24]

Binding of the octacations $[(2\text{-Mepy})_8PzZn]^{8+}$ and $[(2\text{-Mepy})_8QxPzZn]^{8+}$ to different types of DNA in water solution. As already mentioned in the introduction the new octacationic macrocycles are of interest also as G-quadruplex (G4) ligands. To ascertain their potential in this field we performed a study of the binding of these species in water with different types of DNA, both G4 DNA and model B DNA, affording the binding constants as well as structural information on the complexes formed. In the following we illustrate the datafor the Zn^{II} complex $[(2\text{-Mepy})_8PzZn]^{8+}$, a better singlet oxygen producer than the related Mg^{II}complex $[(2\text{-Mepy})_8PzMg(H_2O)]^{8+}$, this latter suffering from chemical instability in the K^+ rich phosphate buffer (see Figure S1 in SI for some binding data of the Mg^{II} complex). To ascertain systematically the role played by the dimension of central aromatic core, the study has been completed with an investigation of the DNA binding of the largercation $[(2\text{-Mepy})_8QxPzZn]^{8+}$with a central π-conjugated aromatic plane of ca. 17 Åmarkedly different from the ca. 8 Åof $[(2\text{-Mepy})_8PzZn]^{8+}$and all new data were compared with those already discussed[8]for the Zn^{II} pyrazinoporphyrazine octa- and hexacations shown in Scheme 1B,C with an aromatic core of intermediate dimension, *ca.* 13 Å. The latter species can form stable 2:1 and 1:1 porphyrazine:G4complexes with the sequence 5'-d[AGGG(TTAGGG)$_3$]-3' (hTel22) adopting a "parallel" G4 structure. Likely efficient π-π stacking of the porphyrazines with the top and/or bottom tetrad in the complex is promoted by the similar dimension of the π-conjugated central macrocyclic framework [27] and the tetrads of the G4 structure (12.0-12.5 Å).[28]Being the size of the aromatic ring similar to that of the G4 tetrad (see Scheme 3 showing relative dimensions of the smaller and intermediate macrocycles and the G4 tetrad), it has been suggested that also electrostatic interactions contributed involving the negatively charged DNA backbone and the peripheral charged pyridines since they can protrude toward the G4 grooves as favoured by their out of plane orientation by ca. 55-60° with respect to porphrazine core.[11]

The binding to different types of DNA for the smaller $[(2\text{-Mepy})_8PzZn]^{8+}$ and larger $[(2\text{-Mepy})_8QxPzZn]^{8+}$ cations has been studied by means of optical spectroscopic techniques.

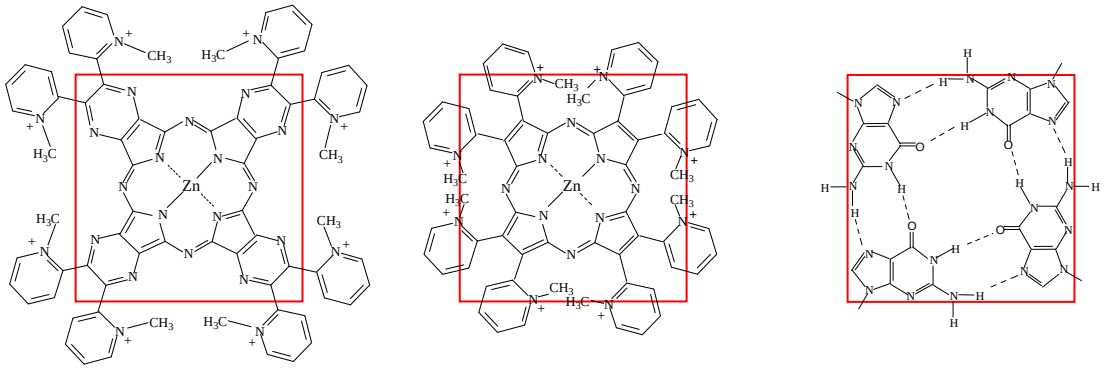

Scheme 3. Illustration of the relative dimensions of the two cations $[(2\text{-Mepy})_8\text{TPyzPzZn}]^{8+}$,$[(2\text{-Mepy})_8\text{PzZn}]^{8+}$ and of a G-tetrad of hTel22.

Binding study of [(2-Mepy)$_8$PzZn]$^{8+}$. Water solutions of $[(2\text{-Mepy})_8\text{PzZn}]^{8+}$at fixed concentration were titrated with varying concentrations of DNA keeping the DNA concentration excess below a factor 5. Three types of DNA were used for the binding experiments: a telomeric sequence adopting a hybrid G4 structure, hTel22,[29,30] the guanine-rich *c-Myc* promoter gene sequence assuming a parallel G4 structure, c-myc2345,[31] and a self complementary sequence, ds26mer, mimicking double-stranded (ds) B DNA upon hybridization.

The absorption spectra of $[(2\text{-Mepy})_8\text{PzZn}]^{8+}$/DNA mixtures in buffered solution were registered in the 210-850 nm interval, while multiwavelength global analysis of the data concerned the 350-840 nm range where the signal observed is exclusively due to the porphyrazine. Also in this KCl-rich buffer the absorption spectrum of $[(2\text{-Mepy})_8\text{PzZn}]^{8+}$ has the typical features of the monomeric species with maxima at 378 and 643 nm. In all cases interaction with DNA results in a small red shift of both the Soret and Q bands of 5-7 nm and 12-18 nm, respectively, depending on the DNA used (Figure 4a-c-e). The largest shift is observed for interaction of the complex with G4 in parallel conformation. We do not observe any important hypochromicity upon ligand binding to the three types of DNA used in this study. This supports the hypothesis that we can safely exclude intercalation of the cation $[(2\text{-Mepy})_8\text{PzZn}]^{8+}$ between tetrads of the G-quadruplex or base pairs of the ds DNA, which is known to be accompanied by strong hypochromicity in the absorption spectra.[32]This is not surprising considering the presence of eight quaternized 2-pyridyl rings appended to the porphyrazine core likely impeding intercalation.[33]In the case of complexation of $[(2\text{-Mepy})_8\text{PzZn}]^{8+}$ to G4 DNA, convergence of the multiwavelength global analysis was obtained with a binding model consisting in the *exclusive* 2:1 complex (porphyrazine:DNA, Figure 4b-d).

Figure S2 shows nice agreement of the experimental absorbance values with the calculatedvalues at selected wavelengths for the various additions of hTel22. As to binding to the self-complementary sequenceds26mer complexes with 2:1 and 1:1 stoichiometries were obtained (Figure 4f); the self-complementary sequence ds26mer is sufficiently long to perform two complete helical turns that can arrange up to two macrocycles. The binding constants in Table 3 for the [(2-Mepy)$_8$PzZn]$^{8+}$complexes with 2:1 stoichiometry suggest that the cation [(2-Mepy)$_8$PzZn]$^{8+}$ is able to bind both types of DNA, G4 and ds DNA, with quite similar affinity.

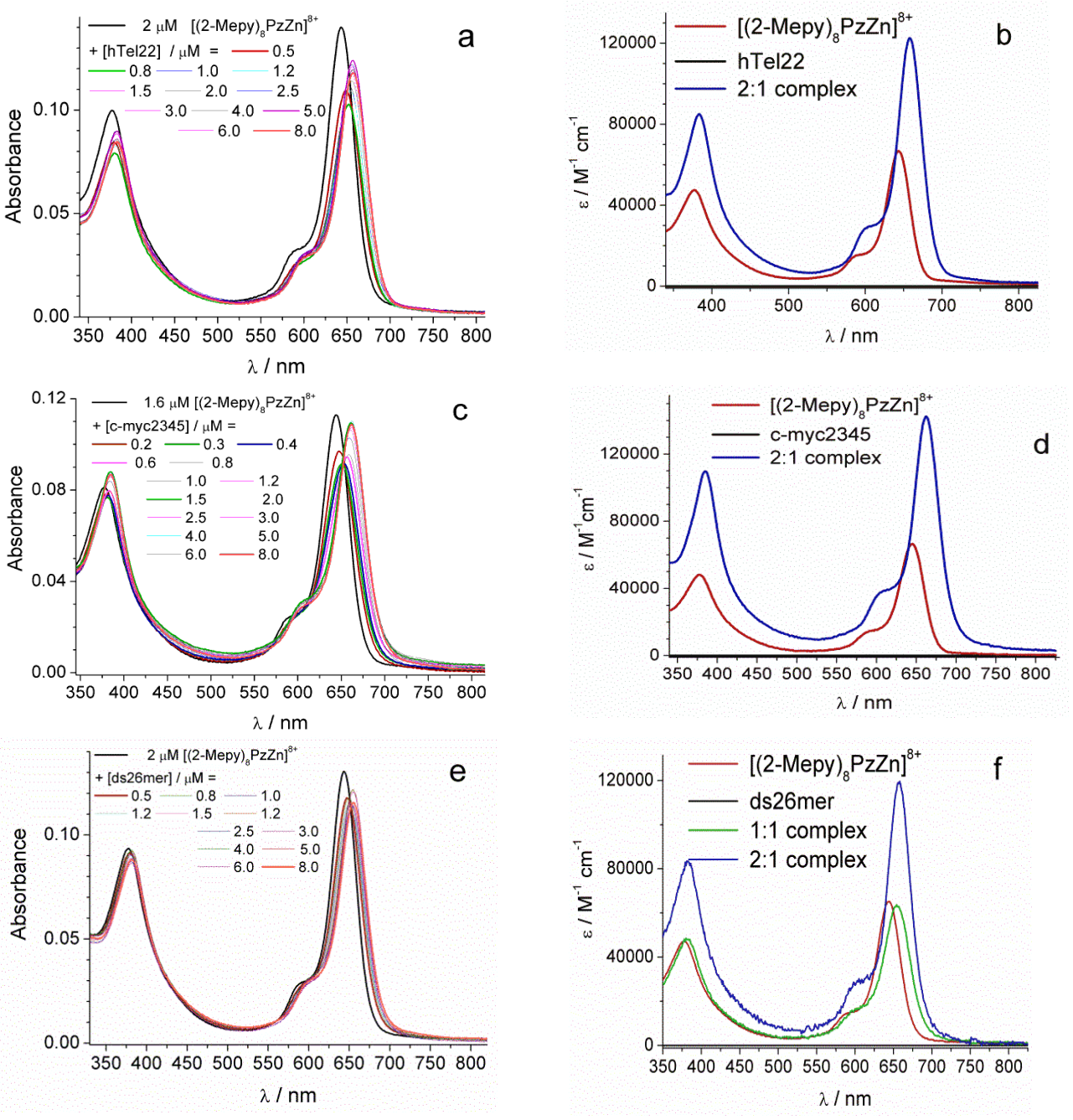

Figure 4. (a) Absorption spectra of solutions [(2-Mepy)$_8$PzZn]$^{8+}$ (2.0×10^{-6} M) with increasing hTel22 concentration (range $0.5\text{-}8\times10^{-6}$ M) in PB/KCl buffer, pH 7.0, d = 1.0 cm; (c) idem, solutions of [(2-Mepy)$_8$PzZn]$^{8+}$ (1.6×10^{-6} M) with

increasing c-myc2345 concentration (range 0.2-8×10^{-6} M); (e) idem, solutions of $[(2\text{-Mepy})_8\text{PzZn}]^8$ (2.0×10^{-6} M) with increasing ds26mer concentration (range 0.5-8×10^{-6} M). (b, d and f) Calculated absorption spectra corresponding to the binding constants with log values 13.04 ± 0.06 and 13.16 ± 0.02 for the 2:1 complex for hTel22 and c-myc2345, respectively, and 6.0 for the 1:1 complex and 12.20 ± 0.06 for the 2:1 complex for the ds26mer (Table 1). Note: the absorption spectrum of the cation $[(2\text{-Mepy})_8\text{PzZn}]^{8+}$ alone is shown in black.

Table 3. Stoichiometry and binding constants obtained from multiwavelength global analysis of the absorption spectra of the mixtures in K^+ rich solutions.

	DNA	**Stoichiometry Ligand:DNA**	**log(K_{11}/M^{-1}), log(K_{21}/M^{-2})[a]**	**log(K_{11}/M^{-1}), log(K_{21}/M^{-2})[b]**
$[(2\text{-Mepy})_8\text{PzZn}]^{8+}$	**hTel22**	2:1	13.04± 0.06	13.33± 0.01[d]
	c-myc2345	2:1	13.16± 0.02	15.11± 0.1
	ds26mer	2:1	12.20± 0.06	12.59± 0.01
		1:1	6.0	6.04±0.01
$[(2\text{-Mepy})_8\text{TPyzPzZn}]^{8+}$	**hTel22**	2:1	14.22± 0.04[c]	
		1:1	6.17± 0.03[c]	
	c-myc2345	2:1	14.81± 0.08[e]	
	ds26mer	2:1	14.30 ± 0.14	
		1:1	5.84 ± 0.08	
$[(2\text{-Mepy})_8\text{QxPzZn}]^{8+}$	**hTel22**	2:1	11.60± 0.06	
		1:1	4.92± 0.15	

[a] K_{21} and K_{11} binding constants, obtained from multiwavelength global analysis of the absorption titration data, with the commercially available program Reactlab Equilibria; [b] K_{21} andK_{11} binding constants, obtained from multiwavelength global analysis of the fluorescence titration data, with the commercially available program Reactlab Equilibria; [c] on basis of absorption data including the dimerization equilibrium of $[(2\text{-Mepy})_8\text{TPyzPzZn}]^{8+}$; lower values of the binding constants K_{21} and K_{11}were reported in ref 8a, obtained from visible Circular Dichroism data without considering the dimerization equilibrium; [d] Convergence has been obtained also for a model with two complexes with stoichiometry 2:1 and 1:1: the program affords log(K_{21}/M^{-2}) = 13.44 ± 0.01 and log(K_{11}/M^{-1}) = 6.33 ± 0.03 being both complexes almost non-emissive; [e] Unpublished data, see also Figure S8.

Binding has also been monitored exploiting the fluorescence of $[(2\text{-Mepy})_8\text{PzZn}]^{8+}$ in the presence of variable amounts of DNA. In 0.01 M aqueous phosphate buffer of pH 7.0 with 0.1 M KCl at 295 K the cation exhibits a fluorescence spectrum characterized by one main band peaking at 665 with a tail extending up to 850 nm (black curve in Figure 5a)and a fluorescence lifetime of 2.2 ns. The fluorescence quantum yield is 0.19, a value indicative of the presence of the monomeric species of

[(2-Mepy)$_8$PzZn]$^{8+}$ and very appealing for optical imaging applications.[34]This emission is completely quenched upon addition of G4 DNA and partially in the case of ds DNA. Fluorescence excitation spectra in the presence of DNA confirm that emission comes from residual free porphyrazine (See Figure S3) as it exhibits the same maximum as porphyrazine in the absence of DNA. Figure 6a shows the fluorescence titration data of [(2-Mepy)$_8$PzZn]$^{8+}$ in the presence ofincreasing concentration of hTel22. In agreement with the data from the absorption spectra, multiwavelength global analysis of the fluorescence spectra converged with a binding model with only the 2:1 complex and afforded a similar binding constant with $\log(K_{21}/M^{-2}) = 13.33 \pm 0.01$. Global analysis afforded a fluorescence quantum yield of the 2:1 complex below 0.1%, so fluorescence is almost completely quenched in the complex. Also in the case of c-myc2345 convergence was obtained with a model consisting in the exclusive 2:1 complex, also with quenched emission. As can be seen in Table 3, the binding constant of the fluorescence data in this case is higher than that of the related absorption data. This difference might be due to unspecific binding in complexes with higher stoichiometry. Indeed, it is possible that electrostatic interaction between positively charged pyridines and the phosphate sugar DNA backbone keeps the Zn^{II} macrocycle and the DNA together reducing the fluorescence intensity due to their vicinity without significantly affecting the absorbanceof the porphyrazine.In the case of ds26mer we needed a binding model with 2:1 and 1:1 complexes, with the latter one resulting to be emissive, in line with the absorption data. An electron transfer process, most likely from the guanosine residues to the excited porphyrazine, might be the reason for fluorescence quenching as documented already in previous literature.[35]The driving force for this photoinduced electron transfer (eT) process can be estimated from the Gibbs free energy equation below, where E_{ox} is the oxidation potential of the electron donor, E_{red} is the reduction potential of the electron acceptor, $E_{0\text{-}0}$ is the singlet excited state energy of the porphyrazine.[36]

$$\Delta G^{eT} = (E_{ox} - E_{red}) - E_{0\text{-}0}$$

We can calculate a value of $E_{0\text{-}0}$ of 15400 cm^{-1}, considering the fluorescence onset at 650 nm or 1.9 eV. The value of E_{ox} ($G^{\bullet+}$/G) is +1.47 V *vs.* NHE.[37]A solution of [Py$_8$PzZn] showed a first reduction at -0.186V *vs.* NHE. Likely the first reduction potential of the relative octacation is at less negative values. We can thus calculate a driving force for photoinduced electron transfer of ΔG^{eT}= [1.47 - (-

0.186) - 1.90] eV, *i.e.* about -0.24 eV. Given the approximations involved we can say that photoinduced DNA → porphyrazine* eT is likely exergonic. Electron transfer from the octacationic porphyrazine to DNA is unlikely due to the high charge of the latter.

Self-quenching between the porphyrazines in close proximity in complexed DNA species with 2:1 stoichiometrymay also occur and further account for the fluorescence intensity decrease. Fluorescence decays for excitation at 637 nm have been recorded for $[(2\text{-Mepy})_8\text{PzZn}]^{8+}$ alone and in the presence of varying concentrations of DNA and confirmed steady-state data. The compound $[(2\text{-Mepy})_8\text{PzZn}]^{8+}$in the K^+ rich phosphate buffer has a fluorescence lifetime of 2.2 ns. Global analysis of sets of fluorescence decays has been performed in all cases with a biexponential fitting function (Figure 5b and eq. 2) yielding a fluorescence lifetime of ca. 2.1 ns and one lifetime of ca. 0.2 nsclose to the instrument resolution. The pre-exponential factors are linearly related to the concentration of the species emitting. Along the series of decays the pre-exponential value of the long lifetime decreases with increasing DNA concentration (See table S1, S2 and S3) and it can be assigned to the residual free $[(2\text{-Mepy})_8\text{PzZn}]^{8+}$species. The short lifetime of 0.10 ns and 0.15 ns for G-quadruplex DNA and 0.24 ns for ds DNA has anincreasing pre-exponential with increasing DNA concentration and is likely due to complexed $[(2\text{-Mepy})_8\text{PzZn}]^{8+}$ with a low fluorescence quantum yield as mentioned above. In the case of G4 DNA the average fluorescence lifetime obtained from eq. 4 decreases from 2.20 ns of the free $[(2\text{-Mepy})_8\text{PzZn}]^{8+}$species to 1.33 ns for the hTel22 complex and 1.14 ns for the c-myc2345 complex while for ds DNA the average fluorescence lifetime is hardly decreasing (See tables S1, S2 and S3) since the pre-exponential factor of the long lifetime decreases to a less extent in ds DNA complexes compared to the G4 complexes. This is indicative of the presence of a second species, most likely complexed, with a lifetime similar to that of free porphyrazine. To rationalize this behavior we envisage different complexation modes.Stacking of the cationic macrocycle with the G-tetrad occurs at short distances of few Å and can favor electron transfer quenching processes thus shorthening the lifetime of the macrocyle in this position. Binding consisting in groove interaction likely occurring both in G4 and ds DNA complexes may give origin to complexed species with a longer lifetime being the porphyrazine at further distance from the guanines.[38] The strongest increase in the pre-exponential value of the short lifetime is indeed observed for the c-myc2345 parallel G4 with the top and bottom G-tetrad

accessible for stacking. As to self-quenching between porphyrazines in complexes with 2:1 stoichiometry note that the ds26mer sequence can adopt two full turns measuring each ca. 3.4 nm, thus keeping two porphyrazine molecules possibly at rather large distance one from the other and preventing their interaction. In the complexes of the more compact G4 structure with 2:1 stoichiometry the two porphyrazines are likely at shorther distances.[38]

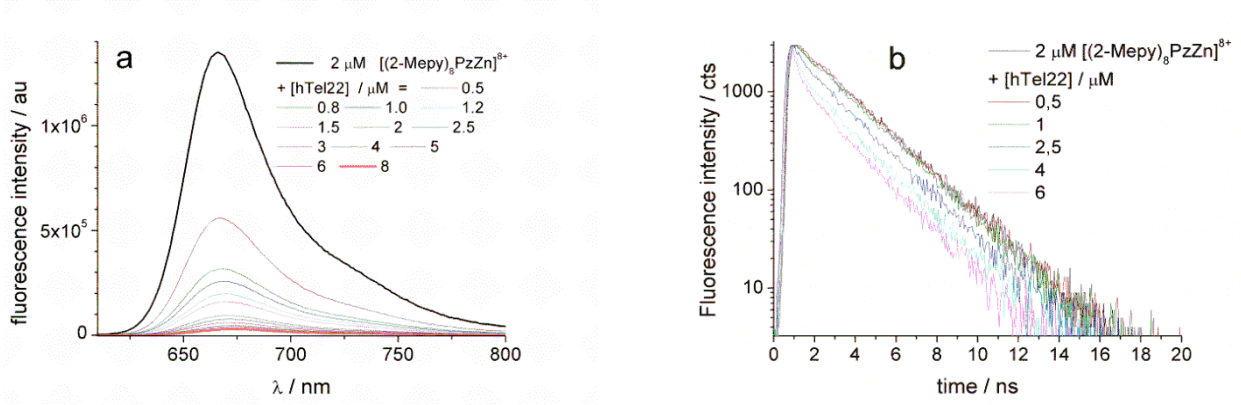

Figure 5. (a) Fluorescence spectra of solutions of $[(2\text{-Mepy})_8\text{PzZn}]^{8+}$ (2.0×10^{-6} M) with increasing hTel22 concentration (range 0.5-8)$\times10^{-6}$ M in PB/KCl buffer, pH 7.0, d = 1.0 cm. Note: fluorescence spectrum of $[(2\text{-Mepy})_8\text{PzZn}]^{8+}$ alone is represented black. (b) Fluorescence decay of solutions of $[(2\text{-Mepy})_8\text{PzZn}]^{8+}$ (2.0×10^{-6} M) alone and with some selected hTel22 concentrations. Excitation at 600 nm for spectra and 647 nm for decay.

UV-visible circular dichroism (CD) is a very useful technique to study binding to DNA. The DNA CD signal in the region 210-330 nm changes in the case of hTel22 (Figure 6a), and remains practically unchanged in the case of c-myc2345 (Figure 6c) and ds26mer (Figure S4).The lack of significant changes in the case of c-myc2345 and ds26mer suggests that the DNA structure is not modified upon complexation by $[(2\text{-Mepy})_8\text{PzZn}]^{8+}$. The folded G4 of the sequence hTel22 in K^+ rich buffer exhibits the typical spectral features of a mixture of 3+1 hybrid and basket conformers as main and minor species, respectively (Figure 6a, black curve).[29]The presence of $[(2\text{-Mepy})_8\text{PzZn}]^{8+}$ leads to an intensity increase of the positive shoulder at 275 nm. The reason for this intensity increase, is likely a partial transformation of the hybrid G4 to a parallel G4. This is confirmed by the CD spectra obtained heating the same solutions at 60°C for 20 minutes that show a more intense band at 275 nm compared to the 290 nm band (See figures 6a,b).

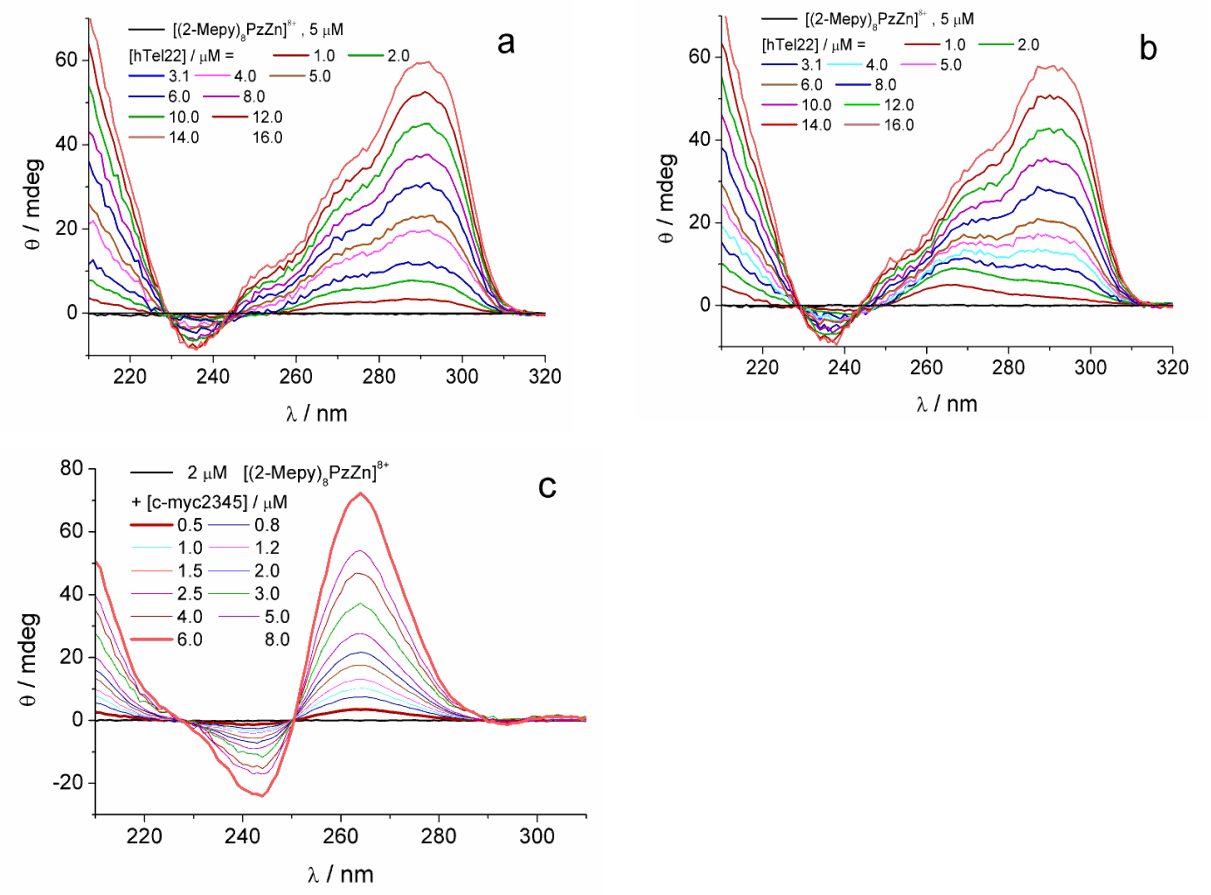

Figure 6. (a) Circular dichroism spectra of solutions of $[(2\text{-Mepy})_8\text{PzZn}]^{8+}$ (5×10^{-6} M) containing increasing concentrations of hTel22 in PB/KCl buffer, pH 7.0; (b) Circular dichroism spectra of solutions of $[(2\text{-Mepy})_8\text{PzZn}]^{8+}$ (5×10^{-6} M) containing increasing concentrations of hTel22 in PB/KCl buffer, pH 7.0 heated for 20 minutes at 60°C; (c) Circular dichroism spectra of solutions of $[(2\text{-Mepy})_8\text{PzZn}]^{8+}$ (2×10^{-6} M) containing increasing concentrations of c-myc2345 in PB/KCl buffer, pH 7.4.

In order to understand the effect of the binding of $[(2\text{-Mepy})_8\text{PzZn}]^{8+}$ on the G4 stability we performed melting experiments for hTel22 monitoring the ellipticity at 295 nm and 260 nm for both hTel22 alone (1×10^{-6} M) and hTel22 in the presence of $[(2\text{-Mepy})_8\text{PzZn}]^{8+}$ (3×10^{-6} M) in 10 mM K-phosphate buffer of pH 7.4. The results are shown in Figure 7a and 7b. Similar experiments on c-myc2345 were not possible since it has a melting point above 80 °C much higher than that of hTel22.

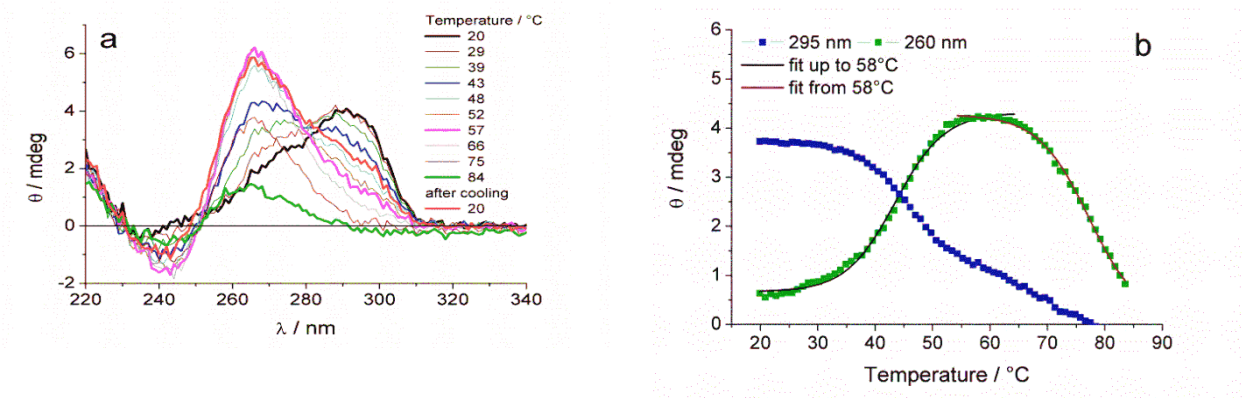

Figure 7. (a) CD spectra of the mixture of $[(2\text{-Mepy})_8\text{PzZn}]^{8+}$ and hTel22 at different temperatures in 10 mM K phosphate buffer of pH 7.0 with 100 mM KCl. (b) Ellipticity changes θ(T) at 295 nm (■) and 260 nm (■) of a mixture of hTel22 (1.0×10^{-6} M) and $[(2\text{-Mepy})_8\text{PzZn}]^{8+}$ (3.0×10^{-6} M) in 10 mM K phosphate buffer of pH 7.0 with 100 mM KCl. Temperature was changed 1°C every 5 minutes.

The folded sequence hTel22 in K^+ rich solution melts at *ca.* 65 ±2 °C, in agreement with data reported in literature (see ESI, Figure S5).[8a,b]The mixture $[(2\text{-Mepy})_8\text{PzZn}]^{8+}$/hTel22 with more than 90% of hTel22 present as 2:1 complex presents instead two transition points in the melting curve. We calculated the first temperature derivative dθ/dT from the data in Figure7 to evidence the melting temperatures. Two melting temperatures around 45 °C and 75 °C emerge but are not well evidenced. Applying a Boltzmann sigmoidal fit to the two parts of the melting curve two inflection points are found. The first one at 44±1 °C, evidenced both at 268 and 290 nm, and a second one at 77±1 °C evidenced at 268 nm. We also registered the CD spectra of the mixture in the 220-340 nm region at various temperatures (see Figure 7a). It is evident from the spectral evolution that a 2:1 complex with less stable G4 conformation, most likely the (3+1) hybrid one, undergoes a conformational transition assuming the parallel G4 structure, characterized by an intense positive and negative peak at 265 nm and 245 nm, respectively. The CD spectrum of the mixture at 66 °C exhibits almost exclusively the parallel G4 features.[39]Only for temperatures higher than 66 °C the parallel complex starts to disappear, but it is still surviving in part at T = 83 °C. Upon slow cooling the solution maintains the spectral features of the parallel conformation indicating that this G4 complex, once formed, is stable. Eventually a 2:1 complex with the telomeric unit in a "parallel" conformation is found as prevailing species after melting in a solution with excess macrocycle. This is further confirmed by the absorption spectra showing a small extra shift to the red when the solutions are warmed up (see Figure S6). Summarizing these data, the smaller cation $[(2\text{-Mepy})_8\text{PzZn}]^{8+}$has a behaviour paralleling the findings for the larger species of Scheme 1B. Indeed the smaller dimension (ca. 8 Å) of the macrocyclic core of $[(2\text{-Mepy})_8\text{PzZn}]^{8+}$ with respect to that of the intermediate cation $[(2\text{-Mepy})_8\text{TPyzPzZn}]^{8+}$ (ca. 13 Å) does not affect the capacity of the former to induce the formation of a stable "parallel" 2:1 porphyrazin:G4 complex likely promoted by π-π stacking in line with the fluorescence data above. Interestingly, two molecules are required in the case of the small porphyrazine $[(2\text{-Mepy})_8\text{PzZn}]^{8+}$ to induce parallel complex formation while $[(2\text{-Mepy})_8\text{TPyzPzZn}]^{8+}$ is able to form parallel G4 complexes with hTel22 independently of the number of porphyrazines complexing.

As to the visible region of the CD spectra (340-750 nm) complexation of $[(2\text{-Mepy})_8\text{PzZn}]^{8+}$ to both G4 and ds DNA resulted in weak circular dichroism signals (See Figure S7 for hTel22) induced in the non-chiral compound interacting with DNA offering a strong chiral environment. Warming the solutions of $[(2\text{-Mepy})_8\text{PzZn}]^{8+}$with hTel22 causes a change in the visible CD signal, especially when $[(2\text{-Mepy})_8\text{PzZn}]^{8+}$is present in excess corresponding to the presence of parallel G4 complexes (See Figure S7a,b). This behaviour differsfrom that of the pyrazinoporphyrazine cations in Scheme 1, reported previously, exhibiting a strong induced CD signal in the same spectral region. In addition, the latter do not require two porphyrazine units complexing the G4 DNA in order to induce parallel G4 formation as both complexes with 2:1 and 1:1 stoichiometry exist in parallel form.[8] These findings suggest some differences in the interaction of the macrocycles of different sizes with the tetrads of hTel22. As can be observed in Scheme 3, availability of the peripheral pyridine rings of $[(2\text{-Mepy})_8\text{PzZn}]^{8+}$for electrostatic interaction with the negatively charged DNA backbone is somewhat restricted due to the smaller dimension of this macrocycle. The cation/tetrad contact is most probably hindered by the non coplanar position of the pyridine rings in the macrocycle. As a result, these structural aspects may reduce the efficiency of the π-π stacking by slightly extending the distance between the small macrocycle and the tetrads of hTel22. Worth of notice, a parallel situation has been reported for the 2:1 complex of the tetracationic compound (N-methyl-4-pyridyl) porphine (TMPyP4) where the steric hindrance imposed by the quaternized pyridine rings directed almost perpendicularly to the plane of the macrocycle raised the distance up to 4.2 Å as established by NMR work.[40]

Binding studies on the octacation $[(2\text{-Mepy})_8\text{QxPzZn}]^{8+}$. Finally we report the binding behaviour of the large cation $[[(2\text{-Mepy})_8\text{QxPzZn}]^{8+}$. Figure 8a shows the absorption spectra we obtain upon addition of increasing amounts of hTel22. It is clear that this complex behaves in a completely different way compared to the smaller complexes. Aggregation of the macrocycle is dominating even in the presence of excess DNA. Differently, for the compound with the intermediate macrocyle DNA both in the G-quadruplex and the duplex form was able to disrupt the aggregates of the compound and monomerized it as shown in Figure 8b. The fluorescence of $[(2\text{-Mepy})_8\text{QxPzZn}]^{8+}$is completely quenched in buffer (Figure 8c). Addition of hTel22 gives origin to fluorescence turn-on effect even though fluorescence remains very weak. The CD spectra in Figure

8e,f are indicative of interaction of $[(2\text{-Mepy})_8\text{QxPzZn}]^{8+}$ with the hybrid G4 form of the hTel22 sequence without significantly changing the conformation. Indeed the hybrid features are dominating in all mixtures for the fresh solutions. The same mixtures kept in the dark for 24 hrs give similar spectra except for a positive shoulder at 270 nm typical of parallel G4 formation gaining little in intensity. All these data taken together suggest that the compound remains mainly aggregated in solution and few cationic units bind as monomers to the G4 structure. We performed a global analysis on the multiwavelength fluorescence data. Convergence of the fitting procedure was obtained with a model comprising two complexes of 1:1 and 2:1 stoichiometry with the calculated spectra shown in Figure 8d. The binding constants (Table 3) are lower than those obtained for the compounds with smaller ringsallowing to conclude that this macrocycle is the worst G4 ligand.

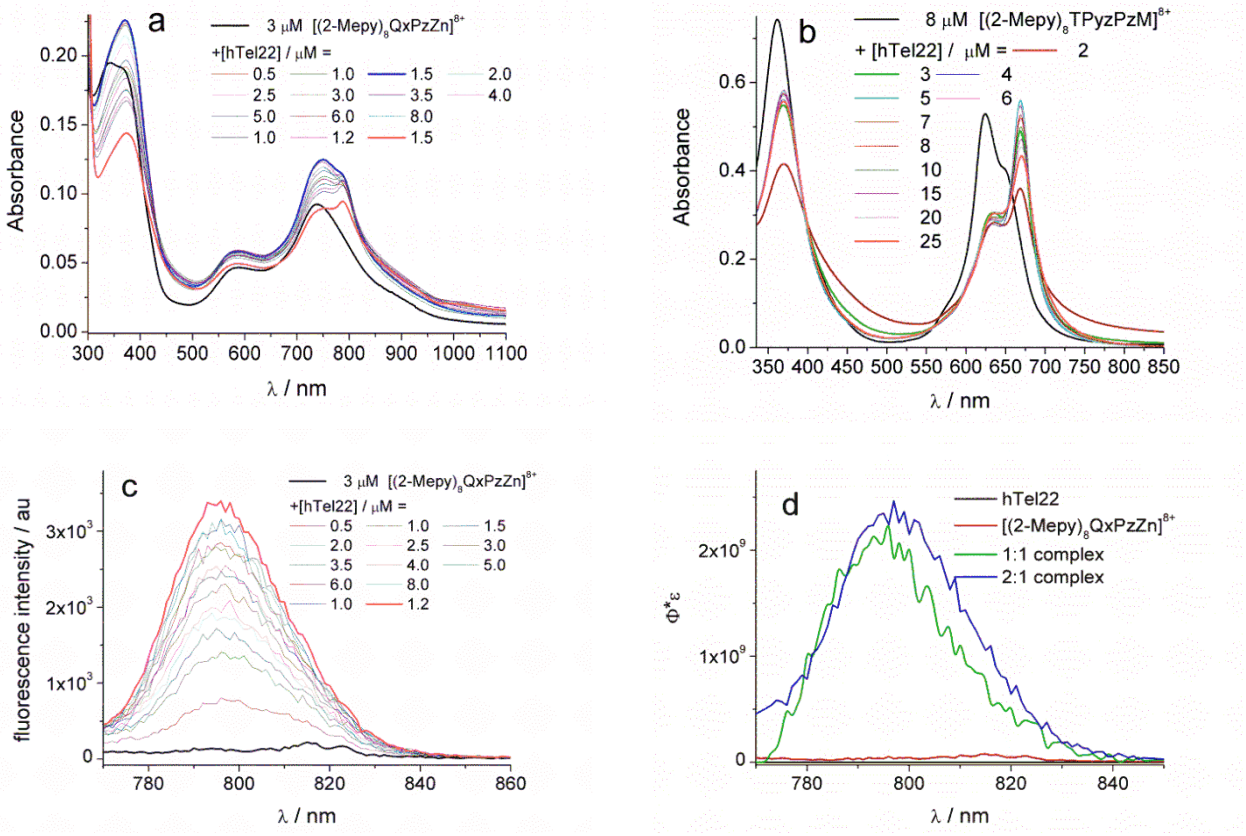

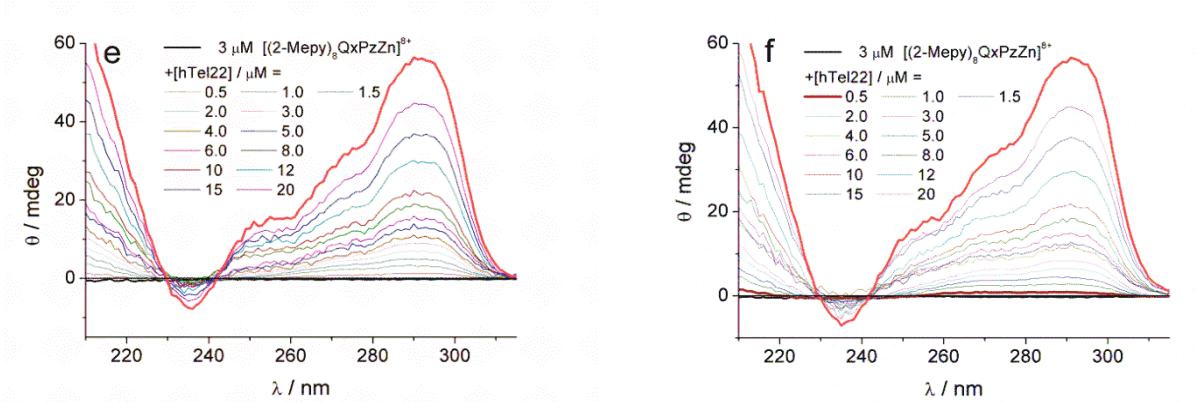

Figure 8: (a) Absorption spectra of solutions $[(2\text{-Mepy})_8\text{QxPzZn}]^{8+}$ (3.0×10^{-6} M) with increasing hTel22 concentration (range 0.5-15.0×10^{-6} M) in PB/KCl buffer, pH 7.4, d = 1.0 cm; (b) idem, solutions of $[(2\text{-Mepy})_8\text{TPyzPzZn}]^{8+}$ (8.0×10^{-6} M) with increasing hTel22 concentration (range 2.0-25.0×10^{-6} M); (c) Fluorescence spectra of solutions $[(2\text{-Mepy})_8\text{QxPzZn}]^{8+}$ (3.0×10^{-6} M) with increasing hTel22 concentration (range 0.5-12.0×10^{-6} M) in PB/KCl buffer, pH 7.4, d = 1.0 cm for excitation at 705 nm. (d) Calculated fluorescence spectra corresponding to the binding constants with log values 4.92 ± 0.14 and 11.60 ± 0.06 for the 1:1 and 2:1 complex of hTel22. (e-f) CD spectra of solutions $[(2\text{-Mepy})_8\text{QxPzZn}]^{8+}$ (3.0×10^{-6} M, fresh solutions and after 24 hrs) with increasing hTel22 concentration (range 0.5-20.0×10^{-6} M) in PB/KCl buffer, pH 7.4, d = 1.0 cm; Note: the absorption spectrum of the cation $[(2\text{-Mepy})_8\text{QxPzZn}]^{8+}$ alone is represented in black.

Summarizing the binding behaviour of the triad of octacationic species $[(2\text{-Mepy})_8\text{PzZn}]^{8+}$, $[(2\text{-Mepy})_8\text{TPyzPzZn}]^{8+}$ and $[(2\text{-Mepy})_8\text{QxPzZn}]^{8+}$, we need to keep their different aggregation behaviour with $[(2\text{-Mepy})_8\text{PzZn}]^{8+}$ being almost exclusively present as monomer while the larger compounds still suffer from aggregation even in the presence of DNA and binding to DNA of dimers has also been proposed.[11] The complexation modes, i.e. stacking to top or bottom G-tetrad of the G-quadruplex, interaction with the loop bases or groove binding promoted by electrostatic interactions, are not identical for these compounds due to the different dimensions of the aromatic porphyrazine rings carrying eight bulky substituents. Importance of the ring size is demonstrated also by the higher binding constants obtained for the compound with the intermediate ring, $[(2\text{-Mepy})_8\text{TPyzPzZn}]^{8+}$, the one matching best the dimension of the tetrad and pushing the pyridine rings toward the DNA grooves. Binding to DNA disrupts the aggregates of $[(2\text{-Mepy})_8\text{TPyzPzZn}]^{8+}$ while it occurs at very low extent for the largest $[(2\text{-Mepy})_8\text{QxPzZn}]^{8+}$ molecule. Taken all together our data show that aromatic macrocycle dimension is an important feature in view of the design of future G4 ligands.

Conclusions

We have reported on the physicochemical properties of the octacationic metal complexes of a porphyrazine with an aromatic core of reduced dimension. They have been compared to those of our previously studied tetrapyrazinoporphyrazinato larger analogues. Noticeably, the octacationic

complexes $[(2\text{-Mepy})_8PzZn]^{8+}$and $[(2\text{-Mepy})_8PzMg(H_2O)]^{8+}$(salted by I^- ions) are present as monomers in water solution which is a very important novelty since porphyrazines in general suffer aggregation in aqueous environment. The molecules were able to sensitize singlet oxygen production with good yields in a non aqueous solvent (DMF) and more importantly also in aqueous solution. Important from the applicative point a view, a stabilization effect has been observed for the complex of $[(2\text{-Mepy})_8PzZn]^{8+}$ with hTel22. Melting of a solution of hTel22 in the presence of excess $[(2\text{-Mepy})_8PzZn]^{8+}$ results in the formation of complexes exclusively exhibiting parallel G4 conformation with a melting temperature above 77°C. Comparing the binding behaviour of all three Zn^{II} complexes with aromatic cores of different dimension we were able to ascertain the importance of the ring size.As to the smallest and intermediate Zn^{II} macrocycles, they exhibit high binding constants for both G4 and ds DNA. Further, they stabilize the G4 structure in the case of telomeric DNA and promote the formation of 2:1 cation/G4 complexes with parallel G4 conformation both favoured by π-π stacking and by electrostatic interactions.The Zn^{II} complex with the central core having the largest dimension superior to that of the G-tetrad is the least efficient ligand.Cytotoxicity and photocytotoxicity studies will be carried out in the next future to evaluate the biological importance of these complexes and further validate the data obtained in solution.

Acknowledgements: Financial support by the University of Rome La Sapienza (Ateneo 2016, B82F16003510005) is gratefully acknowledged.The MIUR (bandiera project NANOMAX-CHEM), the Italian Association for Cancer Research (AIRC, IG2013-14708) and EC (7FP-ITN CyclonHit project n°608407) also financially supported this work.

Author Information

Corresponding Authors:

*E-mail: mariapia.donzello@uniroma1.it

*E-mail: ilse.manet@isof.cnr.it

Notes:

FS and FM equally contributed to this work.

References

(1) P. A. Donzello, M. P.; Ercolani, C.; Novakova, V.; Zimcik, P.; Stuzhin, P. A. Tetrapyrazinoporphyrazines and their metal derivatives. Part I: Synthesis and basic structural information.*Coord. Chem. Rev.* **2016**,*309*, 107-179.

(2) (a) Donzello, M. P.; Ou, Z.; Monacelli, F.; Ricciardi, G.; Rizzoli, C.; Ercolani, C.; Kadish. K. M. Tetra-2,3-pyrazinoporphyrazines with Externally Appended Pyridine Rings. 1. Tetrakis-2,3-[5,6-di(2-pyridyl)pyrazino]porphyrazine: A New Macrocycle with Remarkable Electron-Deficient Properties. *Inorg. Chem.*, **2004**, *43*, 8626-8636. (b) Donzello, M. P.; Ou, Z.; Dini, D.; Meneghetti, M.; Ercolani, C.; Kadish, K. M. Tetra-2,3-pyrazinoporphyrazines with Externally Appended Pyridine Rings. 2. Metal Complexes of Tetrakis-2,3-[5,6-di(2-pyridyl)pyrazino]porphyrazine: Linear and Nonlinear Optical Properties and Electrochemical Behavior. *Inorg. Chem*. **2004**, *43*, 8637-8648. (c) Donzello, M. P.; Viola, E.; Cai, X.; Mannina, L.; Rizzoli, C.; Ricciardi, G.; Ercolani, C.; Kadish, K. M.; Rosa, A.Tetra-2,3-pyrazinoporphyrazines with Externally Appended Pyridine Rings. 5. Synthesis, Physicochemical and Theoretical Studies of a Novel Pentanuclear Palladium(II) Complex and Related MononuclearSpecies.*Inorg. Chem.* **2008**,*47*, 3903-3919. (d) Donzello, M. P.; Viola, E.; Cai, X. H.; Mannina, L.; Ercolani, C.; Kadish, K. M. Tetra-2,3-pyrazinoporphyrazines with Externally Appended Pyridine Rings. 8. Central (Zn^{II}, Cu^{II}, $Mg^{II}(H_2O)$, Cd^{II}) and Exocyclic (Pd^{II}) Metal Ion Binding in Heteropentametallic Complexes from Tetrakis-2,3-[5,6-di(2-pyridyl)pyrazino] porphyrazine. *Inorg. Chem.* **2010**,*49*, 2447-2456. (e) Donzello, M. P.; Viola, E.; Mannina, L.; Barteri, M.; Fu, Z.; Ercolani, C. Tetra-2,3-pyrazinoporphyrazines with externally appended pyridine rings. 11. Photoactivity of a new Pt(II) pentanuclear macrocycle bearing four cisplatin-like functionalities and its related monoplatinated species. *J. Porphyrins Phthalocyanines* **2011,** *15*, 984-994.

(3)Donzello, M. P.; Vittori, D.; Viola, E.; Manet, I.; Mannina, L.; Cellai, L.; Monti, S.; Ercolani, C. Tetra-2,3-pyrazinoporphyrazines with Externally Appended Pyridine Rings. 9. Novel Heterobimetallic Macrocycles and Related Hydrosoluble Hexacations as Potentially Active Photo/ Chemotherapeutic Anticancer Agents. *Inorg*. *Chem*. **2011,** *50*, 7391-7402.

(4) Donzello, M. P.; Viola, E.; Ercolani, C.; Fu, Z.; Futur, D.; Kadish, K. M.Tetra-2,3-pyrazinoporphyrazines with Externally Appended Pyridine Rings. 12. New Heteropentanuclear

Complexes Carrying Four Exocyclic Cis-platin-like Functionalities as Potential Bimodal (PDT/Cis-platin) Anticancer Agents.*Inorg. Chem.* **2012,** *51*, 12548-12559.

(5)Donzello, M. P.; Vittori, D.; Viola, E.; Zeng, L.; Cui, Y.; Kadish, K. M.; Mannina, L.; Ercolani, C. Tetra-2,3-pyrazinoporphyrazines with externally appended pyridine rings. 16. A rare class of uncharged water soluble complexes: UV-vis spectral, redox, and photochemical properties. *J. Porphyrins Phthalocyanines* **2015**, *19*, 903-919.

(6)Bergami, C.; Donzello, M. P.; Monacelli, F.; Ercolani, C.; Kadish, K. M. Tetra-2,3-pyrazinoporphyrazines with Externally Appended Pyridine Rings. 4. UV-Visible Spectral and Electrochemical Evidence of the Remarkable Electron-Deficient Properties of the New Tetrakis-2,3-[5,6-di{2-(N-methyl)pyridiniumyl}pyrazino]-porphyrazinatometal Octacations, [(2-Mepy)8TPyzPzM]$^{8+}$ (M = $Mg^{II}(H_2O)$, Co^{II}, Cu^{II}, Zn^{II}).*Inorg. Chem.* **2005**, *44*, 9862-9873.

(7)Donzello, M. P.; Viola, E.; Bergami, C.; Dini, D.; Ercolani, C.; Giustini, M.; Kadish, K. M.; Meneghetti, M.; Monacelli, F.; Rosa, A.; Ricciardi, G. Tetra-2,3-pyrazinoporphyrazines with Externally Appended Pyridine Rings. 6. Chemical and Redox Properties and HighlyEffective Photosensitizing Activity for Singlet Oxygen Production of Penta- and Monopalladated Complexes in Dimethylformamide Solution.*Inorg. Chem.*, **2008**,*47*, 8757-8766.

(8) (a) Manet, I.; Manoli, F.; Donzello, M. P.; Viola, E.; Andreano, G.; Masi, A.; Cellai, L.; Monti, S. A cationic Zn^{II} porphyrazine induces a stable parallel G-quadruplex conformation in human telomeric DNA. *Org. Biomol. Chem.* **2011**,*9*, 684-688. (b) Manet, I.; Manoli, F.; Donzello, M. P.; Ercolani, C.; Vittori, D.; Cellai, L.; Masi, A.; Monti, S. Tetra-2,3-pyrazinoporphyrazines with Externally Appended Pyridine Rings. 10. A Water-Soluble Bimetallic (Zn^{II}/Pt^{II}) Porphyrazine Hexacation as Potential Plurimodal Agent for Cancer Therapy:Exploring the Behavior as Ligand of Telomeric DNA G Quadruplex Structures.*Inorg. Chem.*, **2011**,*50*, 7403-7411.

(9) (a) Patel, D. J.; Phan, A. T.; Kuryavyi, V.Human telomere, oncogenic promoter and 5'-UTR G-quadruplexes: diverse higher order DNA and RNA targets for cancer therapeutics.*Nucleic Acids Res.* **2007**, *35*, 7429-7455.(b) Burge, S.; Parkinson, G. N.; Hazel, P.; Todd, A. K.; Neidle, S. Quadruplex DNA: sequence, topology and structure. *Nucleic Acids Res.* **2006**,*34*, 5402-5415.(c) Balasubramanian, S.; Neidle, S. G-quadruplex nucleic acids as therapeutic targets. *Curr. Opin. Chem. Biol.* **2009**,*13*, 345-353. (d) Qin, Y.; Hurley, L. H.Structures, folding patterns, and functions

of intramolecular DNA G-quadruplexes found in eukaryotic promoter regions. *Biochimie* **2008**,*90*, 1149-1171.(e) Hurley, L. H. DNA and its associated processes as targets for cancer therapy. *Nat. Rev. Cancer* **2002**,*2*, 188-200. (f) Hurley, L. H. Secondary DNA structures as molecular targets for cancer therapeutics. *Biochem. Soc. Trans.* **2001**, *29*, 692-696.

(10) (a) Chambers**,** V. S.; Marsico, G.; Boutell, J. M; Di Antonio**,** M.; Smith, G. P; Balasubramanian,S. High-throughput sequencing of DNA G-quadruplex structures in the human genome.*Nat. Biotechnol.***2015**,*33*, 877-881. (b)Biffi, G.; Di Antonio, M.; Tannahill, D.; Balasubramanian, S. Visualization and selective chemical targeting of RNA G-quadruplex structures in the cytoplasm of human cells. *Nat. Chem.*, **2014**, *6*, 75-80.

(11)Manet, I.; Manoli, F.; Donzello, M. P.; Viola, E.; Masi, A.; Andreano, G.; Ricciardi, G.; Rosa, A.; Cellai, L.; Ercolani, C.; Monti, S. Pyrazinoporphyrazines with Externally Appended Pyridine Rings. 13. Structure, UV−Visible Spectral Features, and Noncovalent Interaction with DNA of a Positively Charged Binuclear (Zn^{II}/Pt^{II}) Macrocycle with Multimodal Anticancer Potentialities. *Inorg. Chem.***2013**,*52*, 321-328.

(12) Viola, E.; Donzello, M. P.; Sciscione, F.; Shah , K.; Ercolani, C.; Trigiante, G. Tetra-2,3-pyrazinoporphyrazines with externally appended pyridine rings. 17. Photosensitizing properties and cellular effects of Zn^{II} octacationic and Zn^{II}/Pt^{II} hexacationic macrocycles in aqueous media:Perspectives of multimodal anticancer potentialities. *J. Photochem. Photobiol., B: Biology***2017**,*169*, 101-109.

(13)Donzello, M. P.; De Mori, G.; Viola, E.; Ercolani, C.; Ricciardi, G.; Rosa, A. Tetra-2,3-pyrazinoporphyrazines with Externally Appended Pyridine Rings. 15. Effects of the Pyridyl Substituents and Fused Exocyclic Rings on the UV−Visible Spectroscopic Properties of Mg(II)-Porphyrazines: A Combined Experimental and DFT/TDDFT Study. *Inorg. Chem.* **2014**,*53*, 8009-8019.

(14) Sciscione, F.; Cong, L.; Donzello, M. P.;Viola, E.; Ercolani, C.; Kadish, K. M. Octakis(2-pyridyl)porphyrazine and Its Neutral Metal Derivatives: UV−Visible Spectral, Electrochemical, and Photoactivity Studies. *Inorg. Chem.***2017**, *56*, 5813-5826.

(15)Donzello, M. P.; De Mori, G.; Viola, E.; Ercolani, C.; Ricciardi, G. Zinc(II) complexes of tetrakis-(6,7-quinoxalino)porphyrazine bearing externally appended 2-pyridyl rings: Synthesis,

UV-visible spectral behavior and photoactivity for singlet oxygen generation. *J. Porphyrins Phthalocyanines* **2014**, *18*, 1042-1050.

(16) Nyokong, T. Effects of substituents on the photochemical and photophysical properties of main group metal phthalocyanines. *Coord. Chem. Rev*. **2007**, *251*, 1707-1722.

(17)Lukyanets, E. A. Organic Intermediates & Dyes Institute, Moscow 123995, Russia. E-mail: rmeluk@niopik.ru

(18) Kuznetsova, N. A.; Gretsova, N. S.; Derkacheva, V. M.; Kaliya, O. L.; Lukyanets, E. A.Sulfonated phthalocyanines: Aggregation and singlet oxygen quantum yield in aqueous solutions*J. Porphyrins Phthalocyanines* **2003**, *7*, 147-154.

(19) Nyokong, T.; Antunes, E. "Photochemical and Photophysical Properties of Metallophthalocyanines" in *Handbook of Porphyrin Science* **2010**,*7*, 247-357.

(20) Nardello, V.; Brault, D.; Chavalle, P.; Aubry, J. Measurement of photogenerated singlet oxygen ($^1O_2(1\Delta g)$) in aqueous solution by specific chemical trapping with sodium 1,3-cyclohexadiene-1,4-diethanoate. *J. Photochem. Photobiol. B: Biology*, **1997**, 3*29*, 146-155.

(21)Kuznetsova, N. A.; Gretsova, N. S.; Yuzhakova, O. A.; Negrimovskii, V. M.; Kaliya, O. L.; Lukyanets, E. A. New Reagents for Determination of the Quantum Efficiency of Singlet Oxygen Generation in Aqueous Media. *Russ. J. Gen. Chem,* **2001,** *71*, 36-41.

(22) Donzello, M. P.; Viola, E.; Giustini, M.; Ercolani, C.; Monacelli, F.Tetrakis(thiadiazole)porphyrazines. 8. Singlet oxygen production, fluorescence response and liposomal incorporation of tetrakis-(thiadiazole) porphyrazine macrocycles [TTDPzM] (M = $Mg^{II}(H_2O)$, Zn^{II}, $Al^{III}Cl$, $Ga^{III}Cl$, Cd^{II}, Cu^{II}, $2H^{I}$).*Dalton Trans*., **2012**, *41*, 6112-6121.

(23) Maeder, M.; Neuhold, Y-M.in *Practical Data Analysis in Chemistry*, Volume 26, Elsevier Science, **2007**, 1st edition and references therein.

(24) (a) Fernandez, J. M.; Bilgin, M. D.; Grossweiner,L. I. Singlet oxygen generation by photodynamic agents. *J. Photochem. Photobiol. B: Biol*. **1997**, *37*, 131-140. (b) Rosenthal, I.; Murali Krishna, C.; Riesz, P.; Ben-Hur, E. The role of molecular oxygen in the photodynamic effect of phthalocyanines. *Rad. Research* **1986**, *107*, 136-142. (c) Davila, J.; Harriman, A. Photosensitized oxidation of biomaterials and related model compounds. *Photochem. Photobiol*. **1989**, *50*, 29-35. (d) Kuznetsova, N. A.; Gretsova, N. S.; Derkacheva, V. M.; Mikhalenko, S. A.;

Soloveva, L. I.; Yuzhakova, O. A.; Kaliya, O. L.; Lukyanets,E. A. Generation of singlet oxygen with anionic aluminum phthalocyanines in water. *Russ. J. Gen. Chem*. **2002**, *72*, 300-306. (e) Ogunsipe, A.; Nyokong, T. Effects of central metal on the photophysical and photochemical properties of non-transition metal sulfophthalocyanine. *J. Porphyrins Phthalocyanines* **2005,** *9*, 121-129.

(25) Makhseed, S.; Machacek, M.; Alfadly, W.; Tuhl, A.; Vinodh, M.; Simunek, T.; Novakova, V.; Kubat, P.; Rudolf, E.; Zimcik, P. Water-soluble non-aggregating zinc phthalocyanine and in vitro studies for photodynamic therapy. *Chem. Commun*. **2013**, *49*, 11149-11151.

(26) Marti, C.; Nonell, S.; Nicolau, M.; Torres, T. Photophysical properties of neutral and cationic Tetrapyridinoporphyrazines. *Photochem. Photobiol*. **2000**, *7*, 53-59.

(27) Viola, E.; Donzello, M. P.; Ciattini, S.; Portalone, G.; Ercolani, C.Redox Chemistry of Tetrakis[5,6-di(2-pyridyl)-2,3-pyrazino-fused]Porphyrazinato-Cobalt(II): Isolation and Characterization of Solid Pure Co^{I}, Co^{II}, and Co^{III} Complexes. *Eur. J. Inorg. Chem.* **2009**, 1600-1607.

(28) Parkinson, G. N.; Lee, M. P. H.; Neidle, S.Crystal structure of parallel quadruplexes from human telomeric DNA. *Nature* **2002,***417*, 876-880.

(29) Dai, J.; Punchihewa, C.; Ambrus, A.; Chen, D.; Jones, R. A.; Yang, D. Structure of the intramolecular human telomeric G-quadruplex in potassium solution: a novel adenine triple formation. *NucleicAcidsRes.* **2007,** *35*, 2440-2450.

(30) Ambrus, A.; Chen, D.; Dai, J.; Bialis, T.; Jones, R. A.; Yang, D., Human telomeric sequence forms a hybrid-type intramolecular G-quadruplex structure with mixed parallel/antiparallel strands in potassium solution. *Nucleic Acids Res.* **2006,** *34*, 2723-2735.

(31) TuanPhan, A.; Modi, Y. S. ; Patel,D. JPropeller-Type Parallel-Stranded G-Quadruplexes in the Human c-myc Promoter. *J. Am. Chem. Soc.*, **2004**, *12*6, 8710-8716.

(32) (a) Changenet-Barret, P.; Gustavsson, T.; Markovitsi, D.; Manet, I. Ultrafast Electron Transfer in Complexes of Doxorubicin with Human Telomeric G-Quadruplexes and GC Duplexes Probed by Femtosecond Fluorescence Spectroscopy. *Chem. Phys. Chem.***2016**, *17*, 1264-1272. (b) Wan, C.; Xia, T.; Becker, H.-C.; Zewail, A. H. *Chem. Phys. Lett.***2005**, *412*, 158-163.

(33) Freyer, M. W.; Buscaglia, R.; Kaplan, K.; Cashman, D.; Hurley, L. H.; Lewis, E. A., Biophysical Studies of the c-MYC NHE III1 Promoter: Model Quadruplex Interactions with a Cationic Porphyrin. *Biophysical J.* **2007,** *92*, 2007-2015.

(34) (a) To determine the fluorescence quantum yields of the two cationic macrocycles the water-soluble compound ATTO633 has been used as reference with a value of 0.64, see the ATTO catalogue from ATTOTEC GmbH, Germany. (b) Lovell, J. F.; Liu, T. W. B.; Chen, J.; Zheng, G. Activatable Photosensitizers for Imaging and Therapy. *Chem. Rev.* **2010,** *110,* 2839–2857.

(35)Steenkeste, K.; Enescu, M.; Tfibel, F.; Perree-Fauvet, M.; Fontaine-Aupart, M. P.Ultrafast Guanine Oxidation by Photoexcited Cationic Porphyrins Intercalated into DNA. *J. Phys. Chem. B* **2004,** *108*, 12215-12221.

(36) Samir Farid, S.; Dinnocenzo, J. P. ; Merkel, P. B.; Young, R. H.; Shukla, D.; Guirado, G.Reexamination of the Rehm–Weller Data Set Reveals Electron Transfer Quenching That Follows a Sandros–Boltzmann Dependence on Free Energy.*J. Am. Chem. Soc*. **2011**, *133,* 11580–11587.

(37) Seidel, C. A. M.; Schulz A.; Sauer, M. H. M. Nucleobase-Specific Quenching of Fluorescent Dyes. 1. Nucleobase One-Electron Redox Potentials and Their Correlation with Static and Dynamic Quenching Efficiencies. *J. Phys. Chem.*, **1996**, *100*, 5541–5553.

(38) Parkinson, G. N.; Gosh, R.; Neidle, S. Structural Basis for Binding of Porphyrin to Human Telomeres. *Biochemistry***2007**, *46*, 2390-2397.

(39) (a) Bugaut, A.; Balasubramanian, S. A Sequence-Independent Study of the Influence of Short Loop Lengths on the Stability and Topology of Intramolecular DNA G-Quadruplexes. *Biochemistry***2008,***47*, 689-697. (b)Y. Qin, Y.; Hurley, L. H. Structures, folding patterns, and functions of intramolecular DNA G-quadruplexes found in eukaryotic promoter regions. *Biochimie*, **2008,***90*, 1149-1171.

(40) Tuan Phan, A.; Kuryavyi, V.; Yan Gaw, H.; Patel, D. J. Small-molecule interaction with a five-guanine-tract G-quadruplex structure from the human MYC promoter. *Nature Chem. Biol.*, **2005**, 1, 167-173.

Synopsis

The new octacationic Zn^{II} Porphyrazinesolubilizing as monomer in water delivers a promising performance as multimodal agent for therapeutic applications as it is able to photosensitize singlet oxygen formation, emit in the red and stabilize DNA G-quadruplex (G4) structures.